



Microtomographie et paléoneurologie, révélations sur le cerveau des Néandertaliens et sur son fonctionnement ?

Antoine Balzeau

UMR 7194 CNRS, Muséum national d'Histoire naturelle, Paris, France

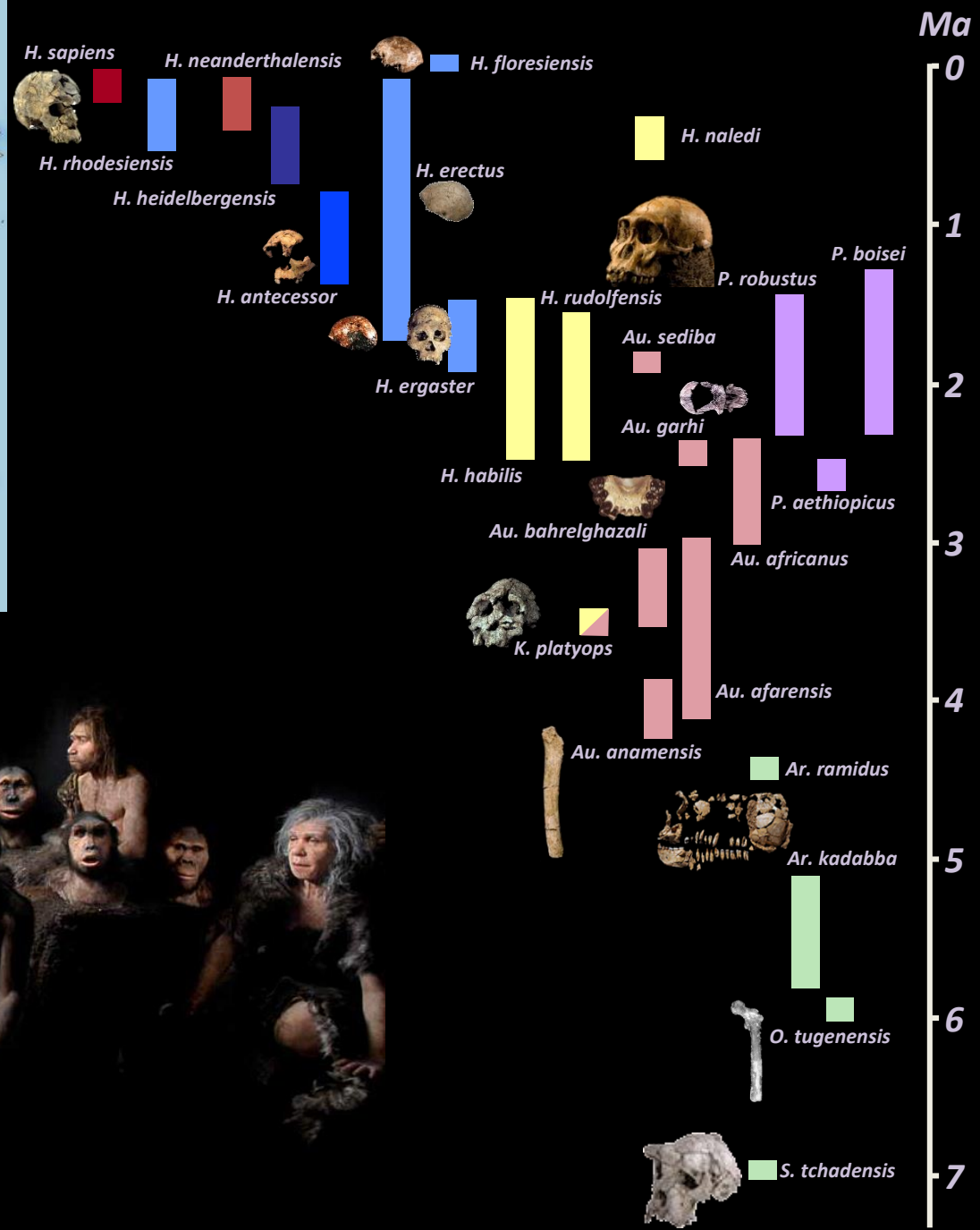
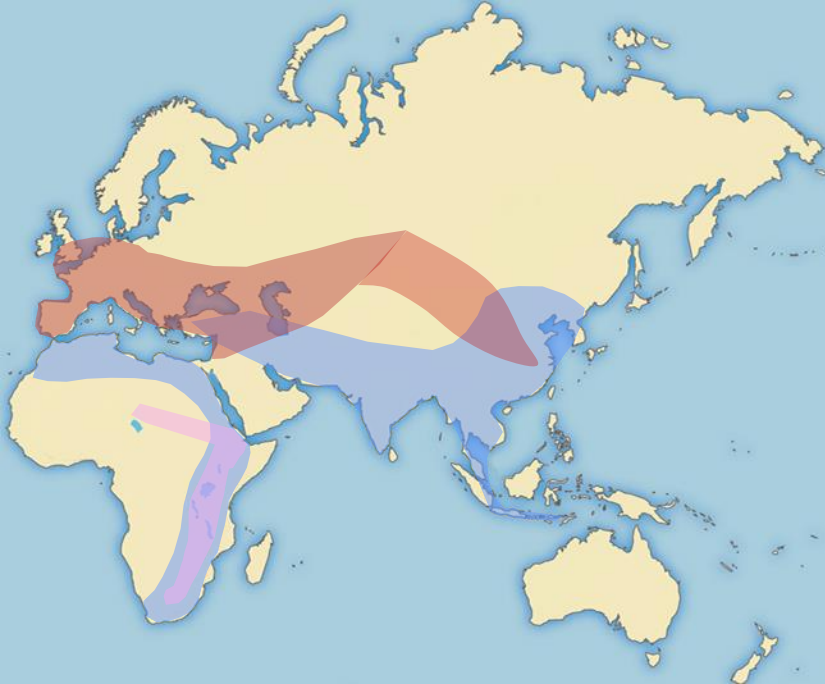
Qui suis-je ?

UMR 7194 CNRS, Muséum national d'Histoire naturelle, Paris, France

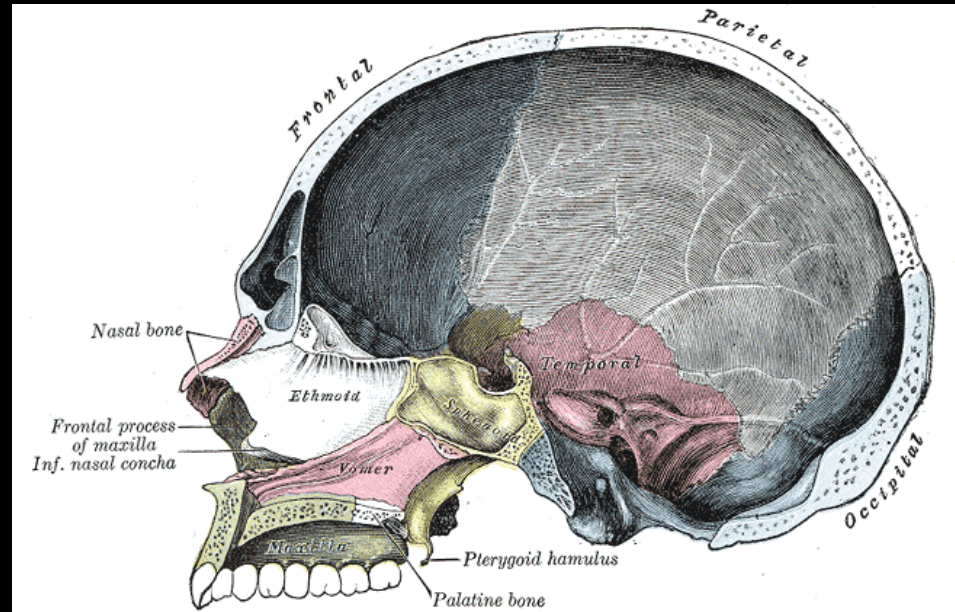


Plate-forme AST-RX, UMS 2700, CNRS-MNHN





Le cerveau, comment étudier ce qui ne se fossilise pas...







L'anthropologie « virtuelle », ou la face cachée des Hommes

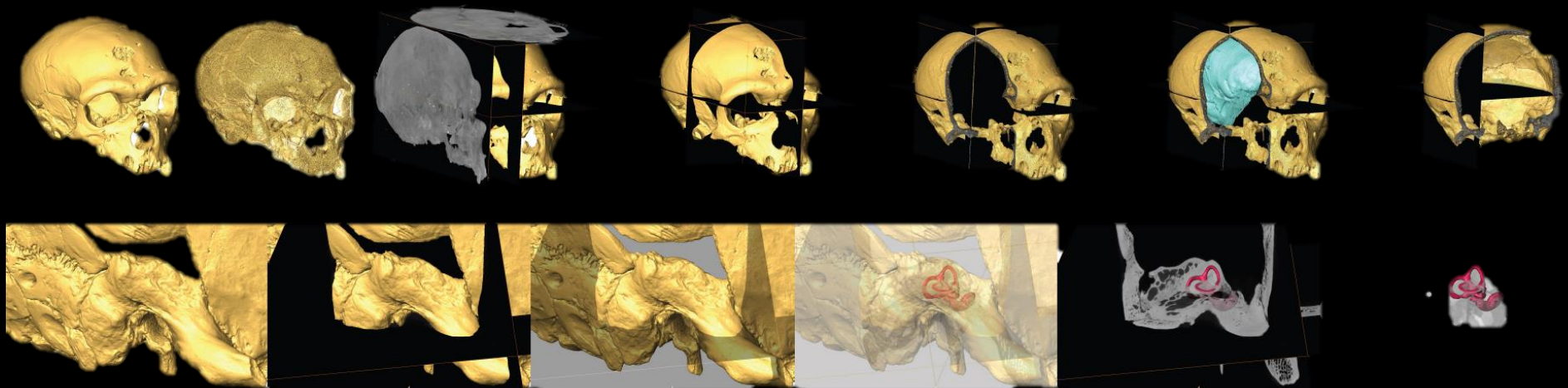


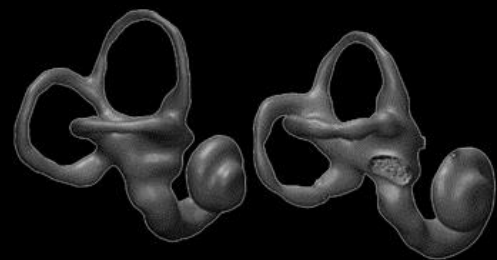
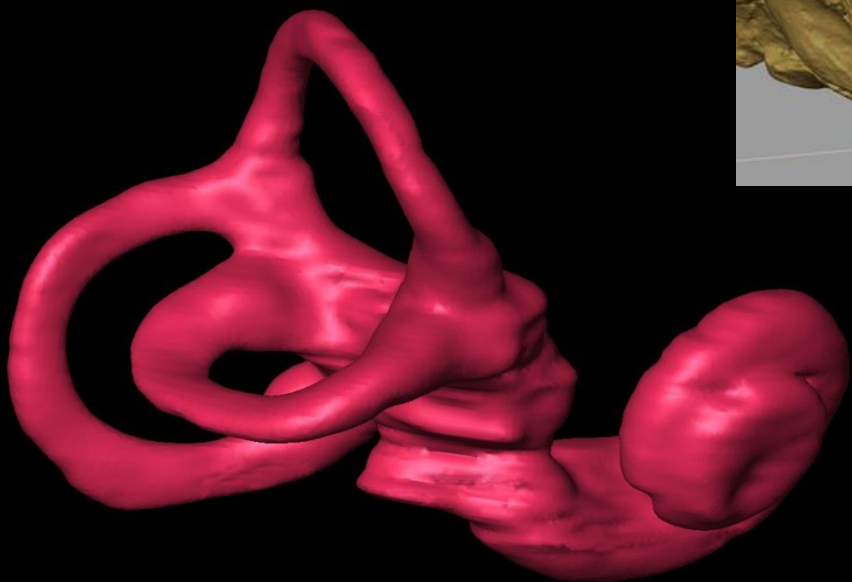
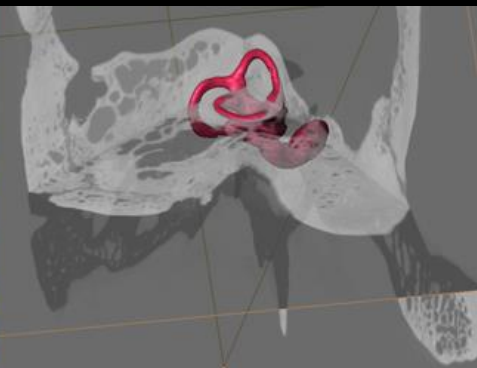
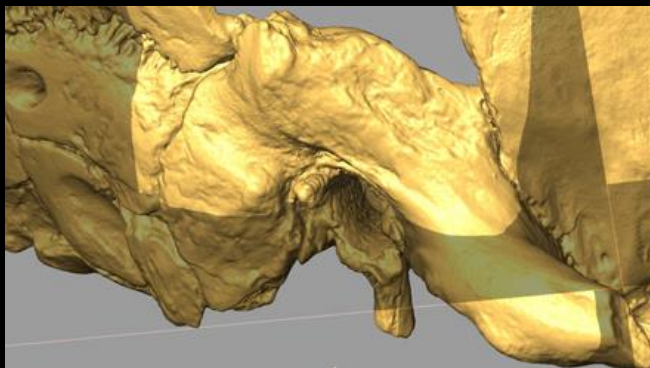
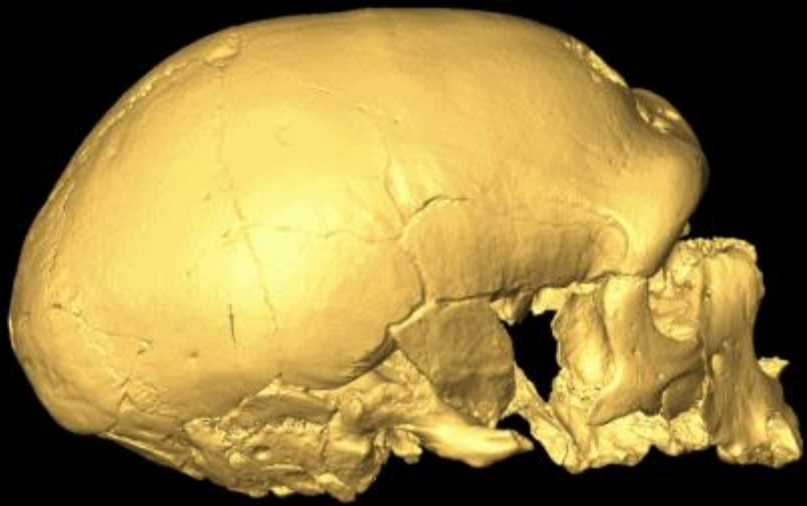
Crâne de Lilian Thuram, *Homo sapiens* actuel Reconstitution 3D, 2006

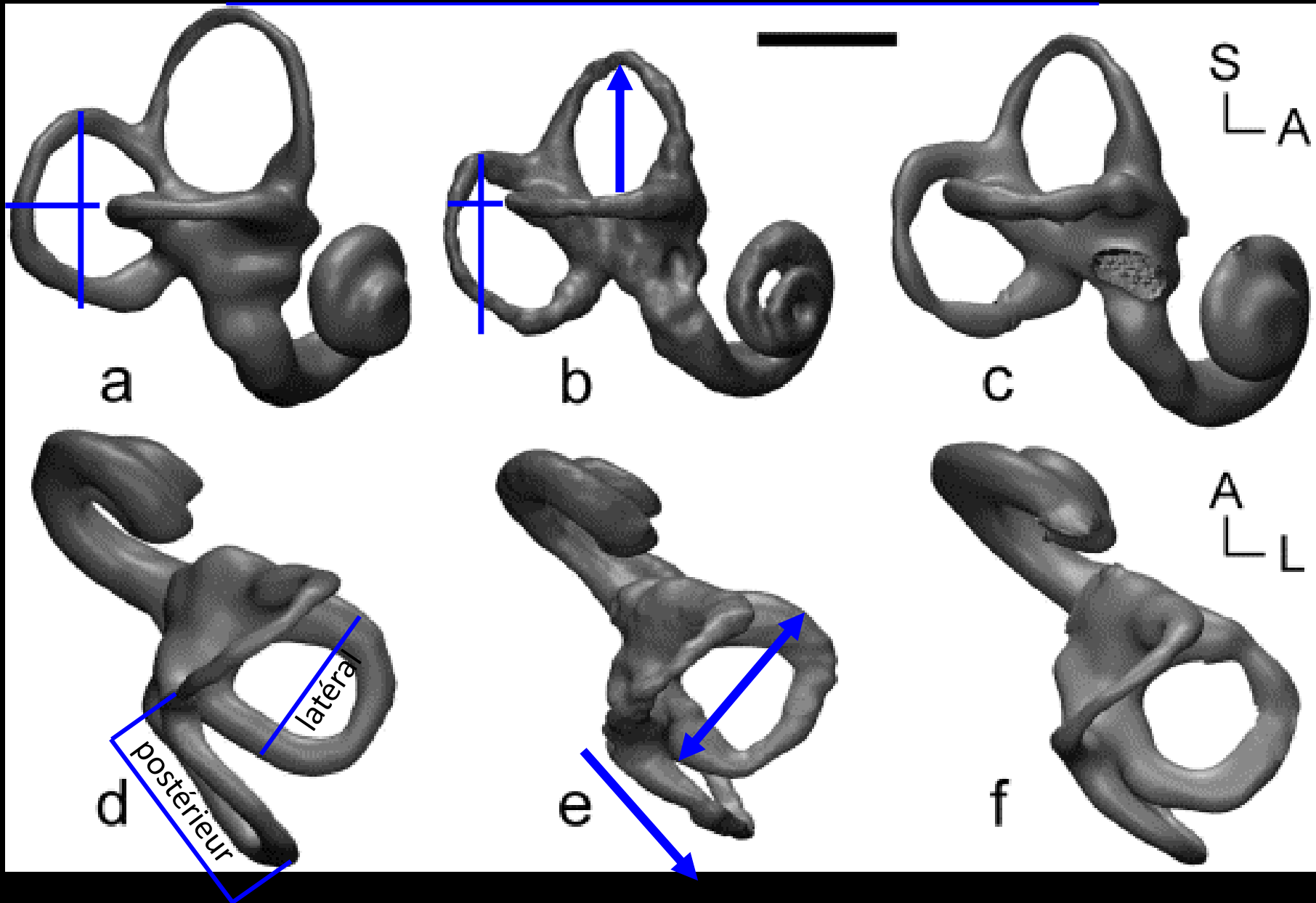
Pour la réalisation de ce crâne, Lilian Thuram a d'abord passé un scanner RX. Les données obtenues ont ensuite subi différents traitements afin d'établir une reconstruction en trois dimensions, en effaçant «virtuellement» la peau, les muscles, etc. À partir de ce crâne virtuel en trois dimensions, un procédé de prototypage a été utilisé pour en fabriquer une réplique exacte. Les traitements des données d'imagerie pour l'obtention de la reconstruction 3D ayant permis la production du prototype ont été effectués grâce au logiciel ArteCore (NESPOS, <https://www.nespos.org>)

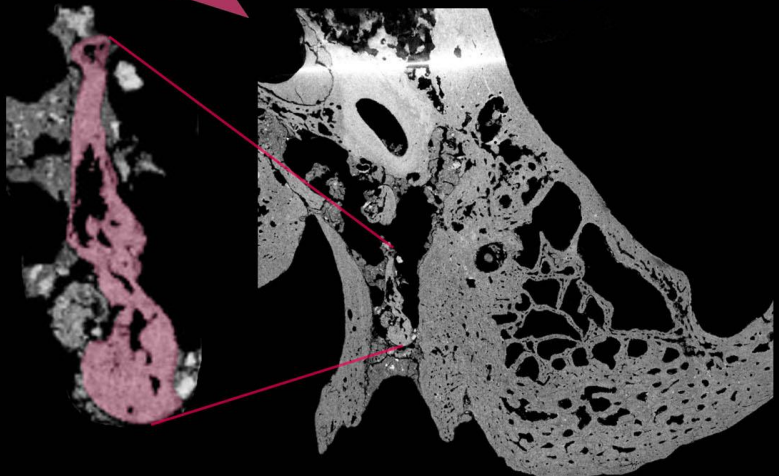
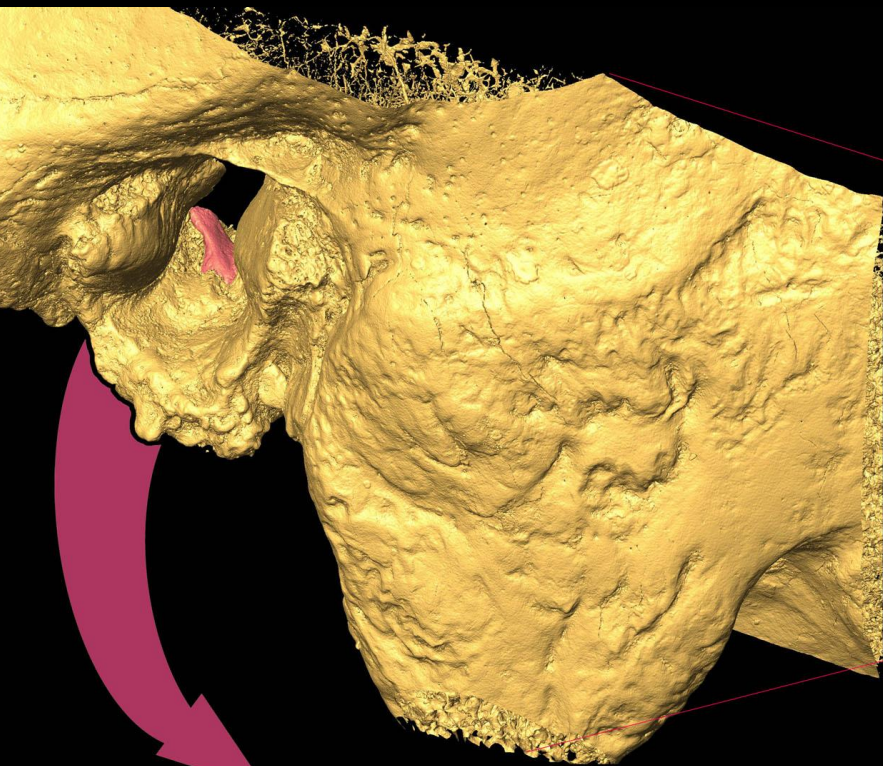
Musée de l'Homme



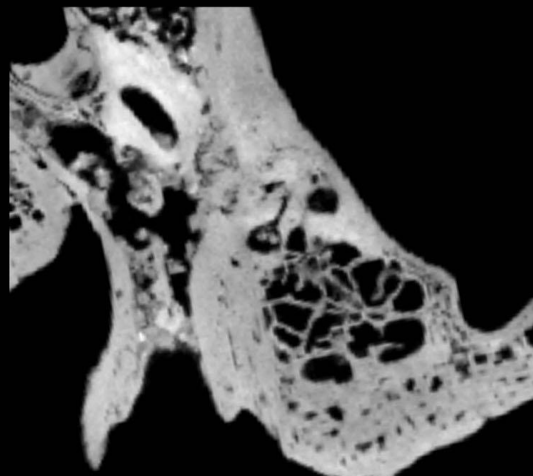




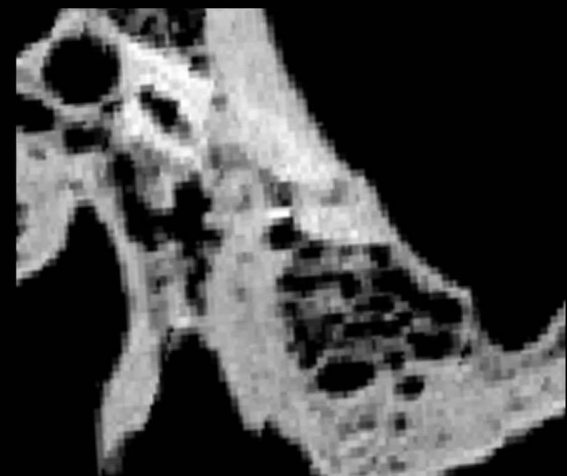




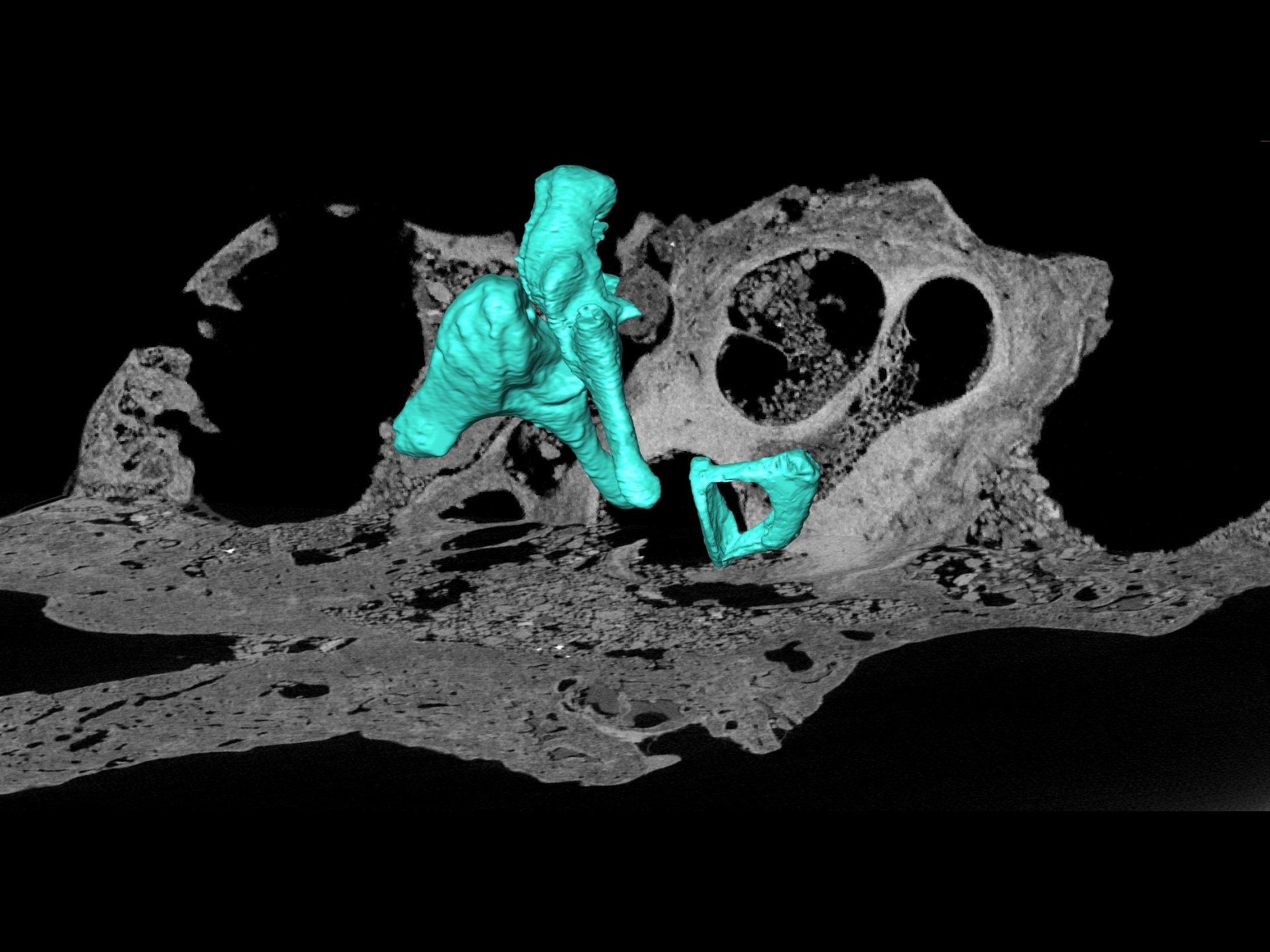
23 microns



123 microns



450 microns



Early hominin auditory capacities
 Quam et al., Science 2015

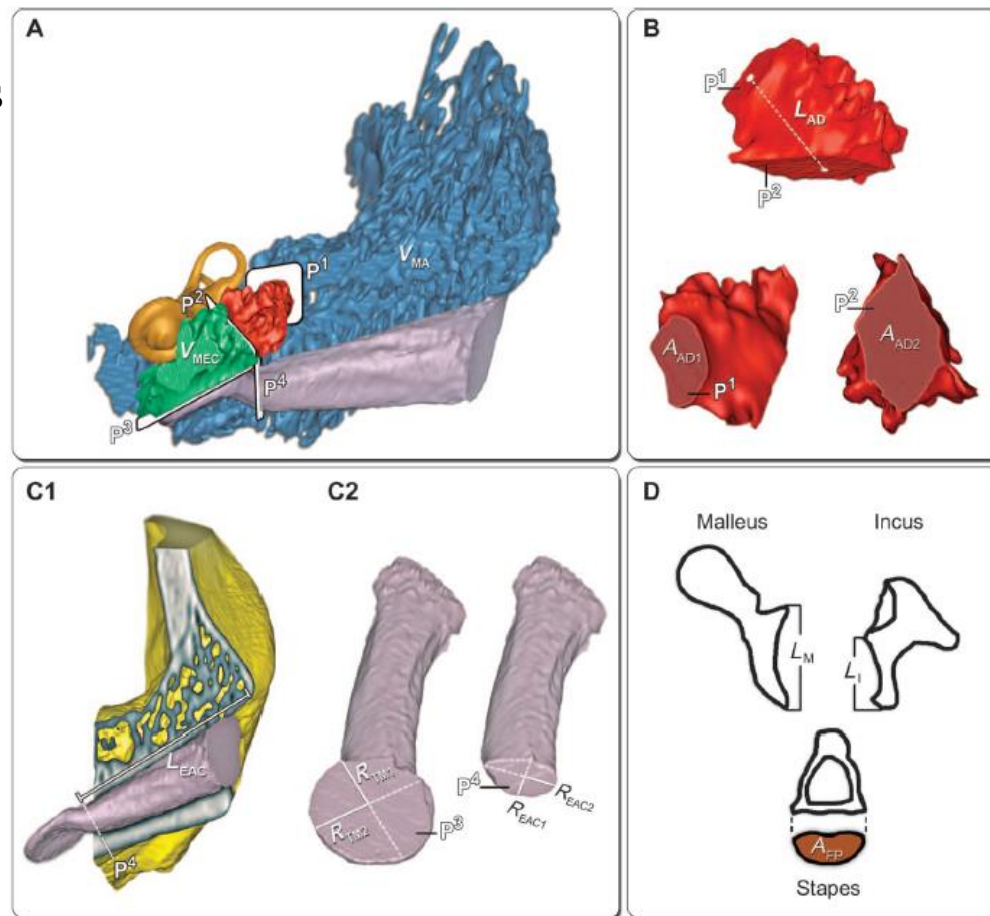
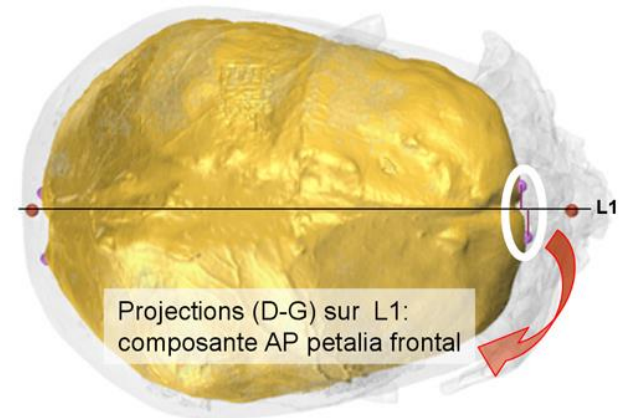
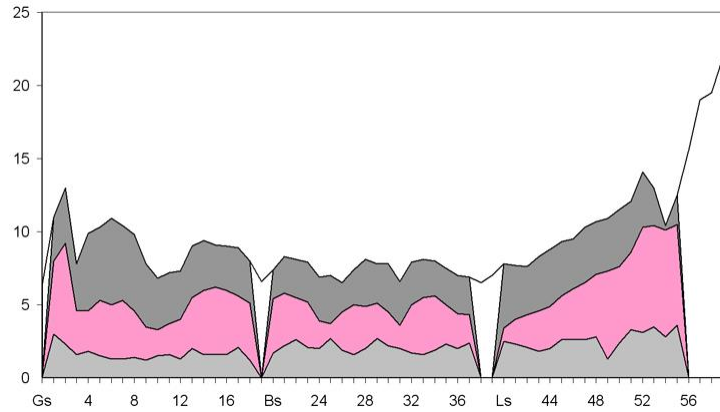
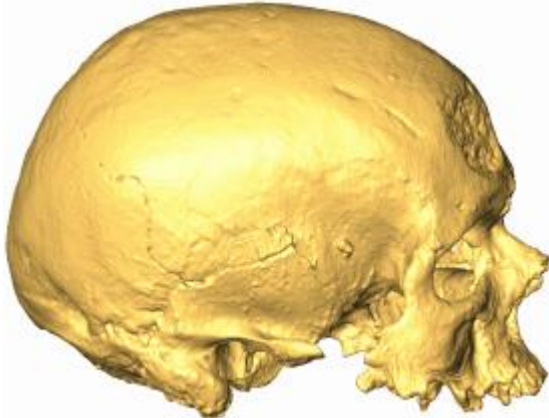
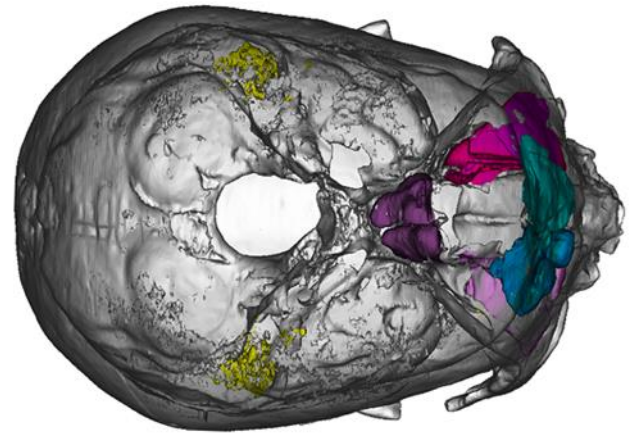
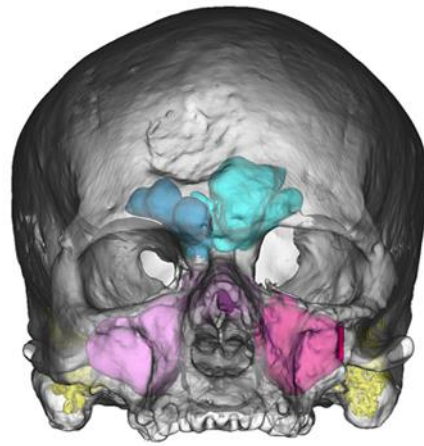
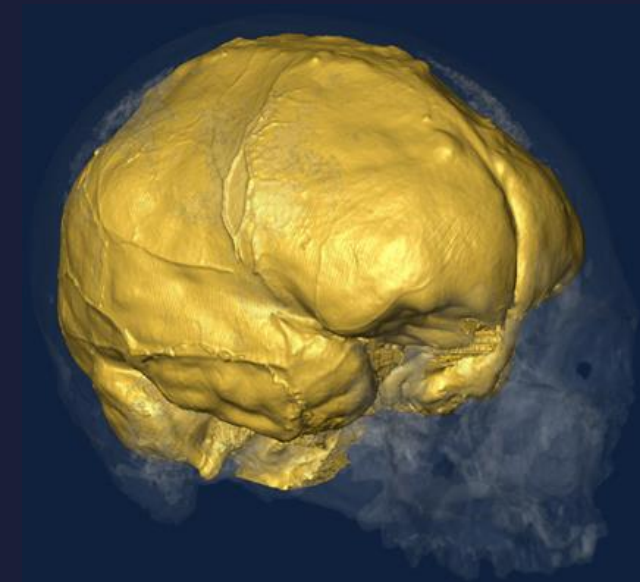
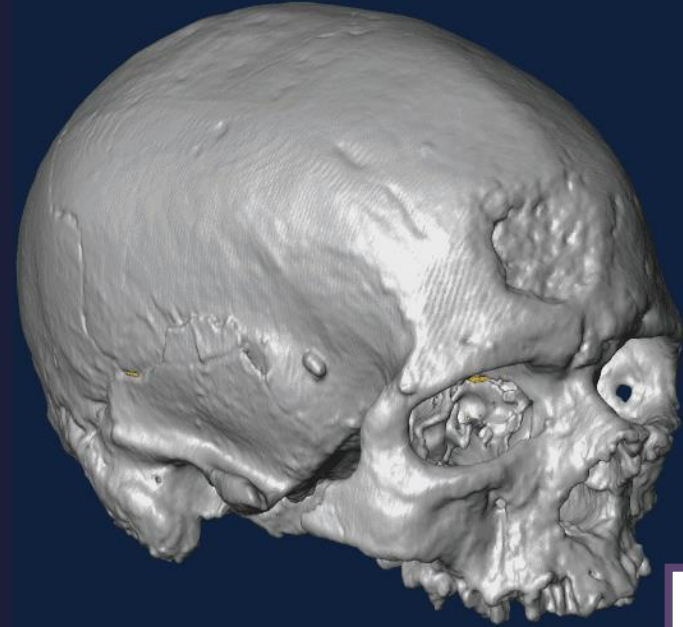
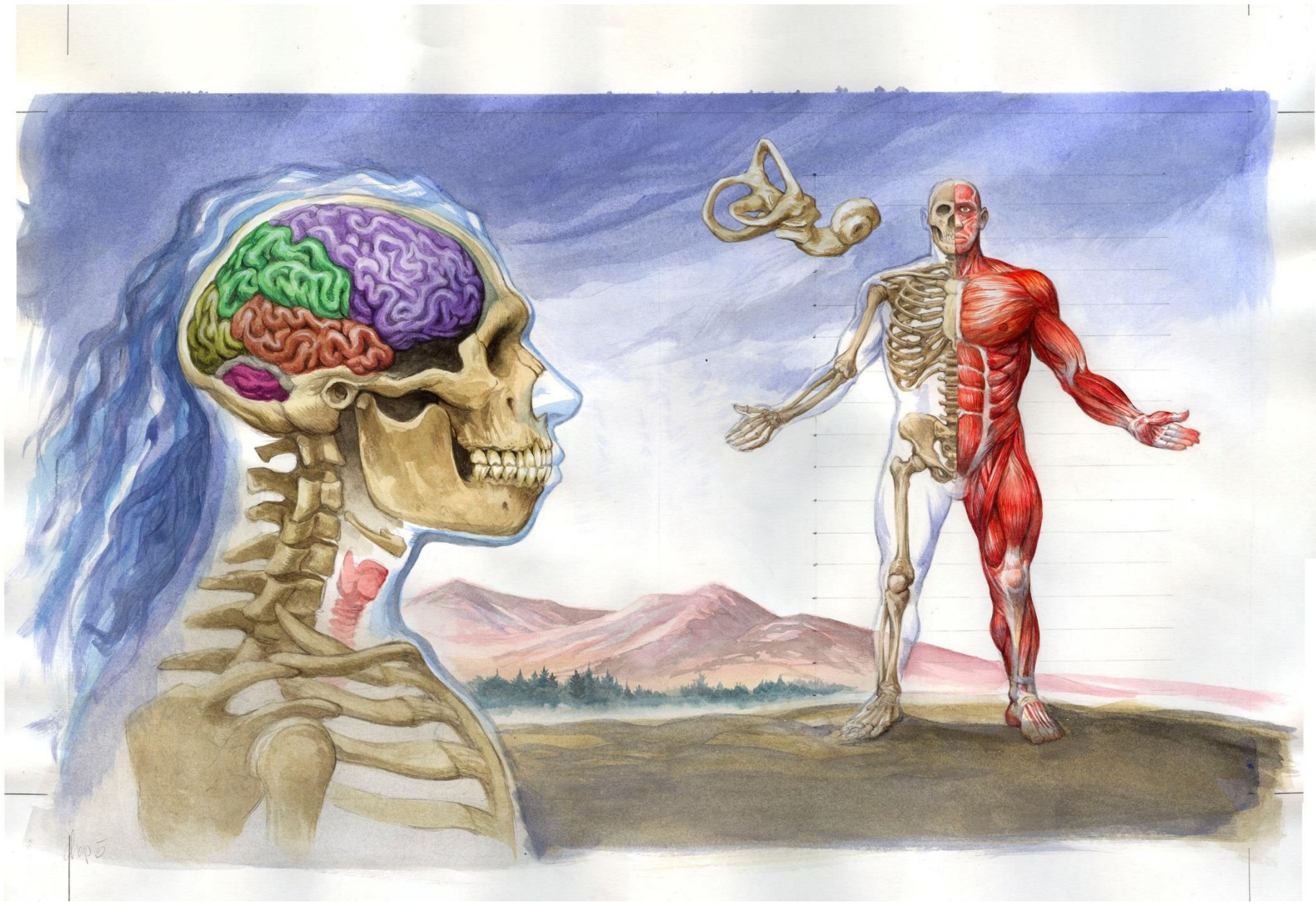


Fig. 1. Measurements of the middle and outer ear (A to C) and ear ossicles (D). (A), (B), (C1), (C2), and (D) are not drawn to the same scale. (A) to (C) are based on the 3D reconstruction of the left side of HTB 1769 (*Pan troglodytes*), showing the EAC (gray), the middle ear cavity (green), the aditus ad antrum (red), the mastoid antrum and connected mastoid air cells (blue), the inner ear (orange), and the temporal bone (yellow). P^1 , limit between the mastoid antrum and the connected mastoid air cells with the aditus ad antrum. P^2 , entrance to the aditus ad antrum from the middle ear cavity. P^3 , medial edge of the tympanic groove (sulcus tympanicus). P^4 , cross section perpendicular to the long axis of the EAC that meets the lateral end of the tympanic groove. (A) V_{MA} , volume of the mastoid antrum and connected mastoid air cells, measured dorsal to P^1 ; V_{MEC} , volume of the middle ear cavity, bounded by P^2 to P^3 . (B) L_{AD} , length of the aditus ad antrum, measured as the distance from the center of P^1 to the center of P^2 ; A_{AD1} , area of the exit of the aditus ad antrum to the mastoid antrum and connected mastoid air cells; A_{AD2} , area of the entrance to the aditus ad antrum from the middle ear cavity. For modeling purposes, we have calculated the radius (R_{AD1} and R_{AD2} ; not shown), which would correspond to a circle with the given area for the exit (A_{AD1}) and entrance (A_{AD2}). (C1) L_{EAC} , length of the EAC, measured from the most lateral extent of the tympanic groove (defined by P^4) to the spina suprameatum. In *Pan*, the spina suprameatum is replaced by the superior-most point of the porus acusticus externus. (C2) R_{TM1} , half of the measured greater diameter of the tympanic membrane, measured in P^3 ; R_{TM2} , half of the measured lesser diameter (perpendicular to R_{TM1}) of the tympanic membrane, measured in P^3 ; R_{EAC1} and R_{EAC2} , half of the measured diameters of the two major perpendicular axes (superoinferior and mediolateral) of the EAC measured at P^4 . (D) is based on the profiles of the malleus and incus from the temporal bone AT-1907 and the stapes from Cranium 5. L_M , functional length of the malleus, measured as the maximum length from the superior border of the lateral process to the stapes from the manubrium; L_I , functional length of the incus, measured from the lateral-most point along the articular facet to the lowest point along the long crus in the rotational axis; A_{FP} , measured area of the footplate of the stapes.

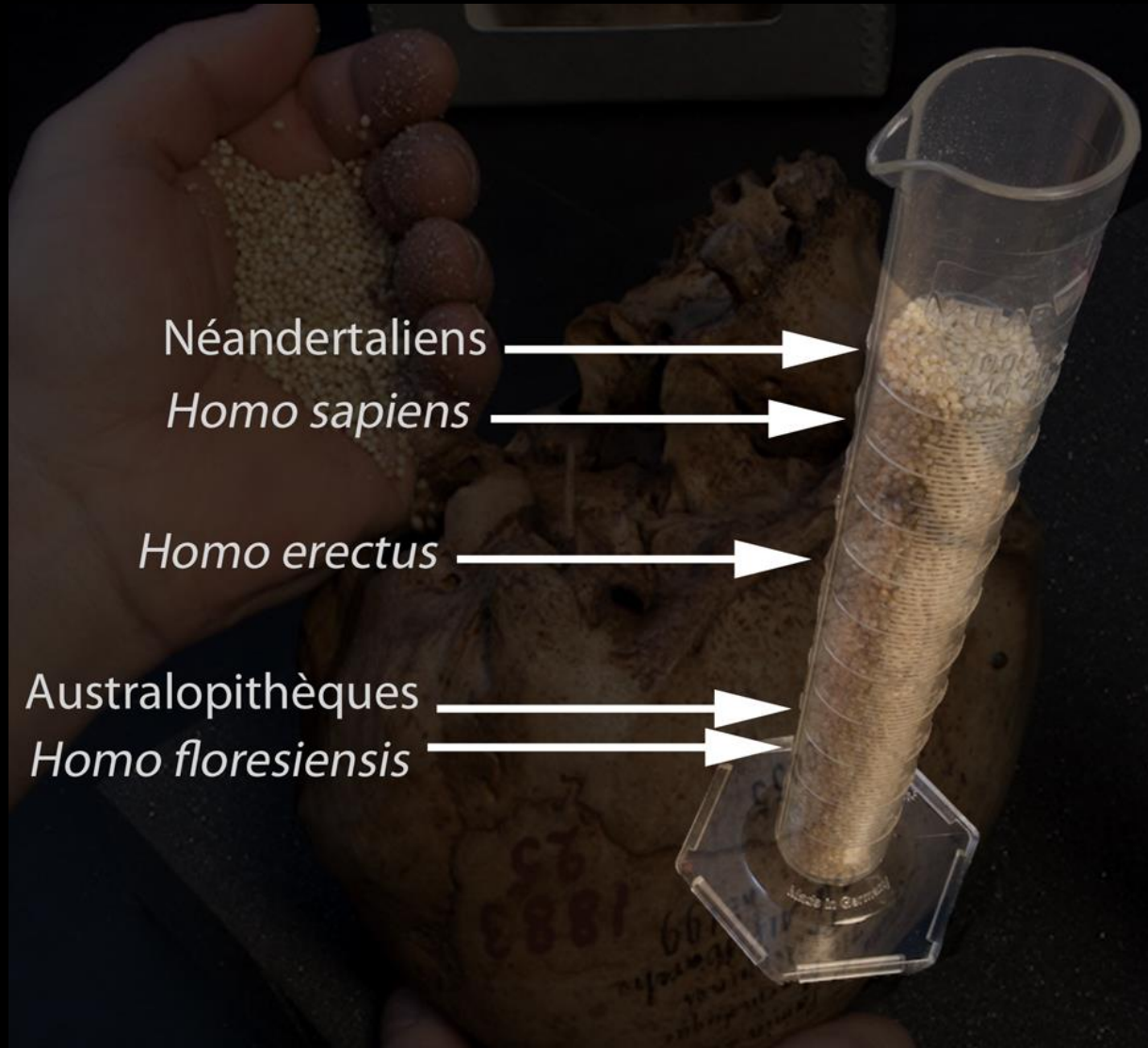


Aller plus loin dans l'exploration : le prototypage rapide

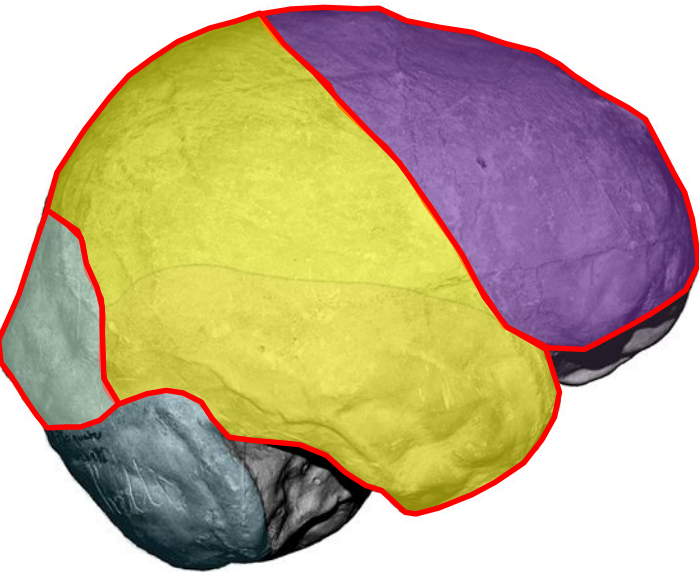
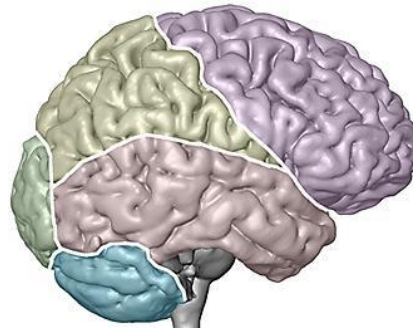
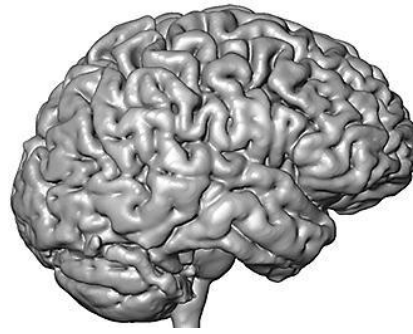




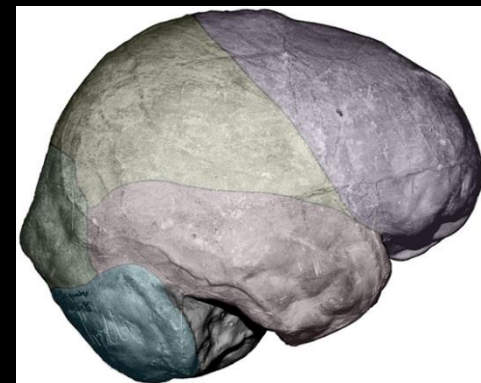
La taille du cerveau...



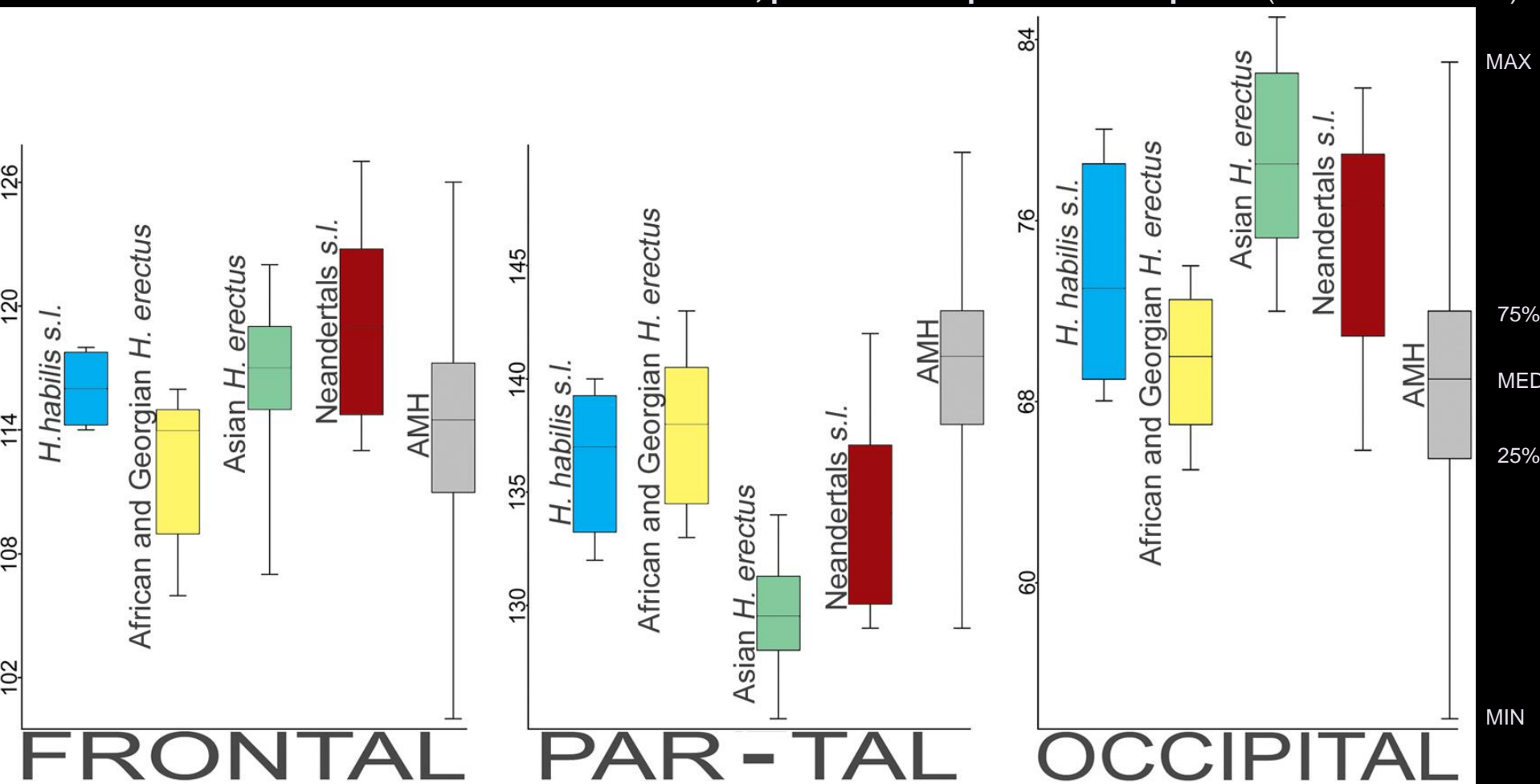
Le « cerveau »



Des différences de forme ?



Variations de la surface des lobes frontaux, pariéto-temporaux et occipitaux (données relatives)





CrossMark
click for updates

Research

Cite this article: Pearce E, Stringer C, Dunbar RIM. 2013 New insights into differences in brain organization between Neanderthals and anatomically modern humans. *Proc R Soc B* 280: 20130168.

<http://dx.doi.org/10.1098/rspb.2013.0168>

Received: 24 January 2013

Accepted: 20 February 2013

New insights into differences in brain organization between Neanderthals and anatomically modern humans

Eiluned Pearce^{1,2}, Chris Stringer³ and R. I. M. Dunbar¹

¹Department of Experimental Psychology, South Parks Road, Oxford OX1 3UD, UK

²Department of Anthropology, University of Oxford, 64 Banbury Road, Oxford OX2 6PN, UK

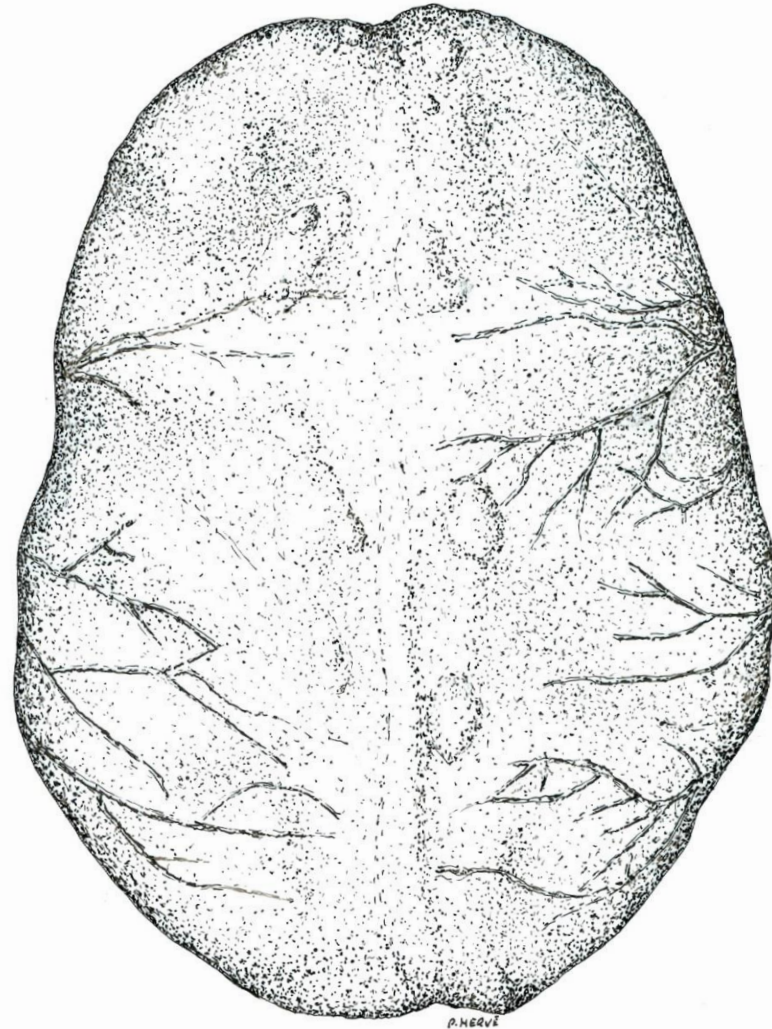
³Natural History Museum, Cromwell Road, London SW7 5BD, UK

Previous research has identified morphological differences between the brains of Neanderthals and anatomically modern humans (AMHs). However, studies using endocasts or the cranium itself are limited to investigating external surface features and the overall size and shape of the brain. A complementary approach uses comparative primate data to estimate the size of internal brain areas. Previous attempts to do this have generally assumed that identical total brain volumes imply identical internal organization. Here, we argue that, in the case of Neanderthals and AMHs, differences in the size of the body and visual system imply differences in organization between the same-sized brains of these two taxa. We show that Neanderthals had significantly larger visual systems than contemporary AMHs (indexed by orbital volume) and that when this, along with their greater body mass, is taken into account, Neanderthals have significantly smaller adjusted endocranial capacities than contemporary AMHs. We discuss possible implications of differing brain organization in terms of social cognition, and consider these in the context of differing abilities to cope with fluctuating resources and cultural maintenance.

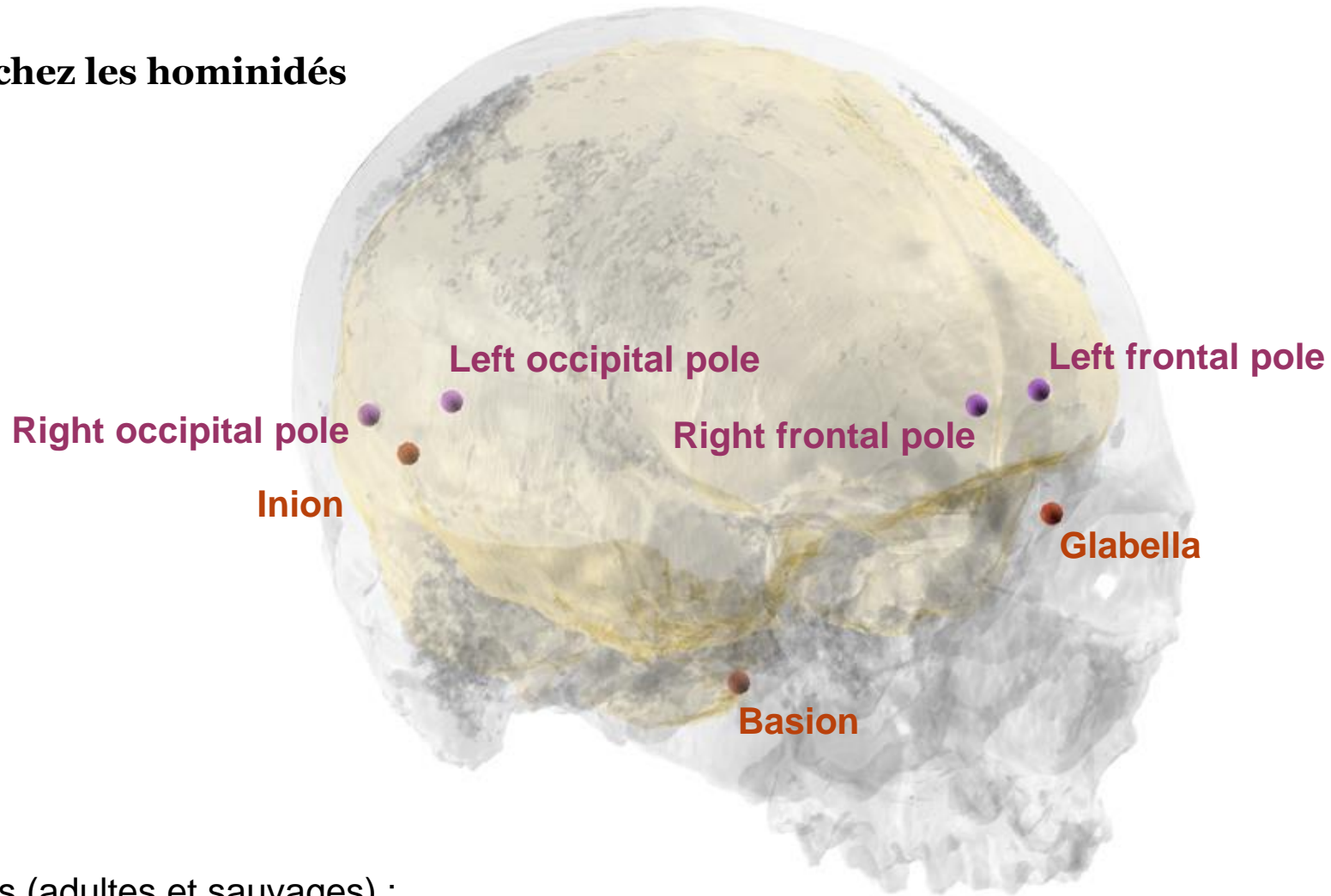


Les pétalias
Et la latéralité manuelle

Plus "l'aire de Broca"



Les pétalias chez les hominidés



110 grands singes (adultes et sauvages) :

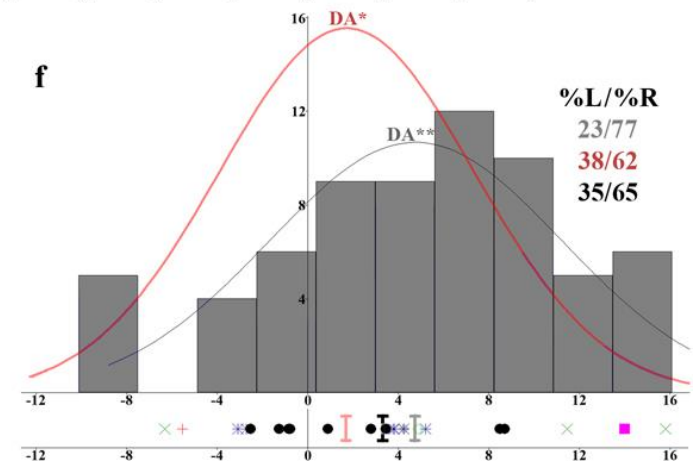
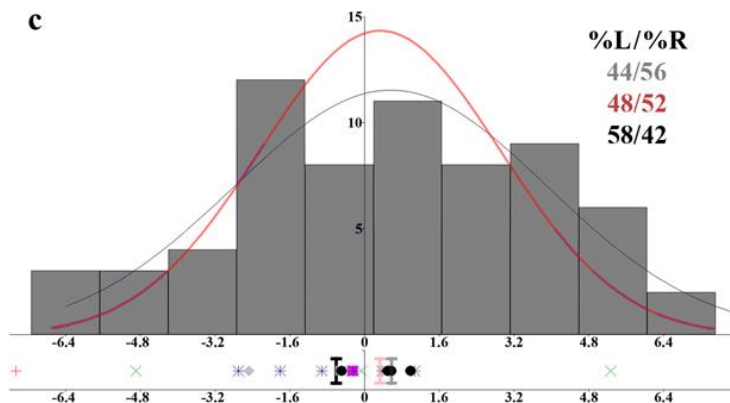
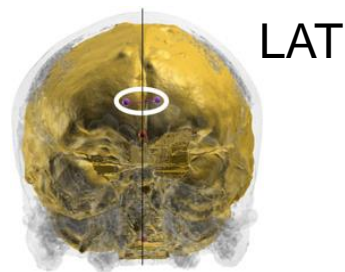
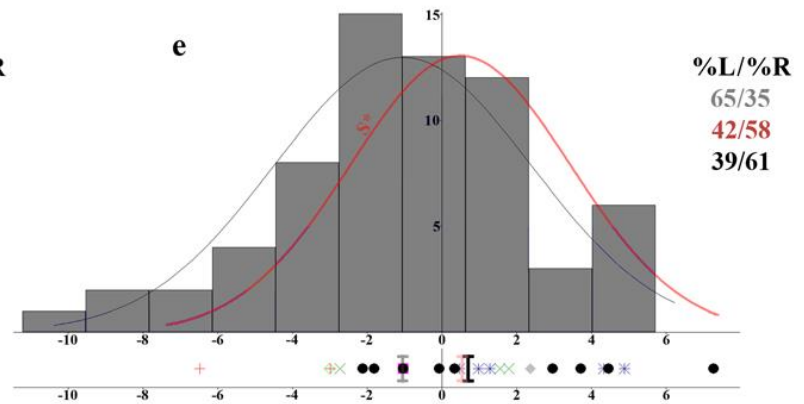
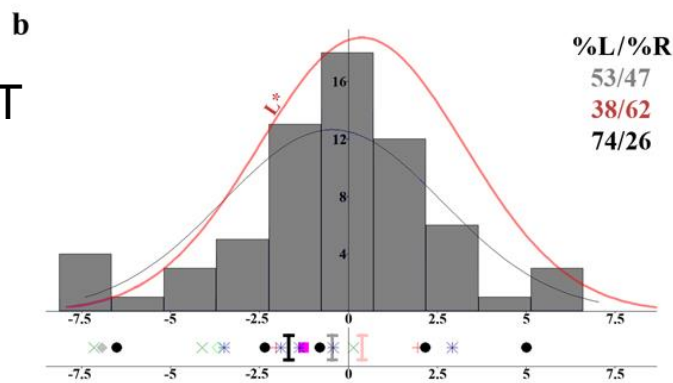
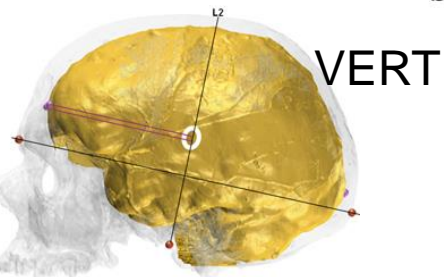
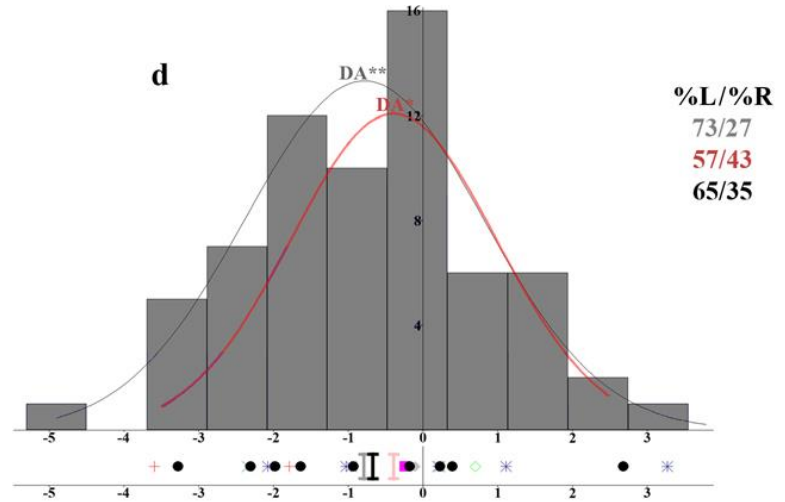
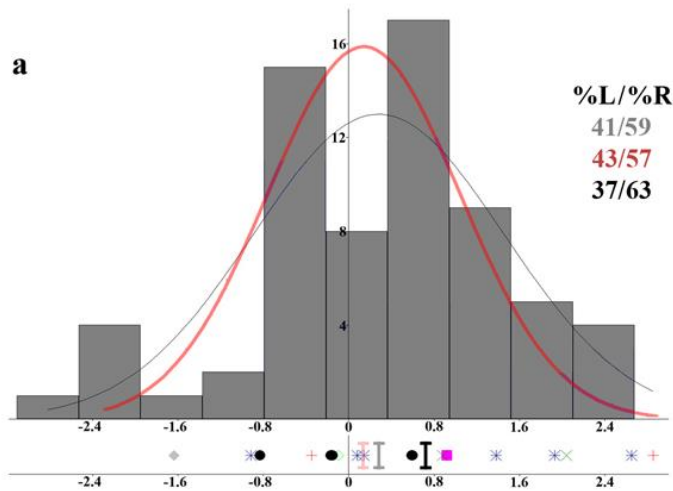
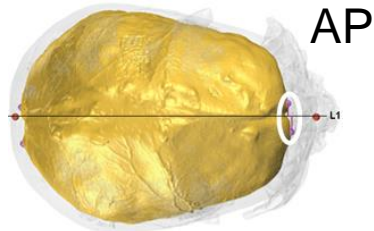
36 *Pan paniscus* (17 mâles/19 femelles), 36 *P. troglodytes* (17/19), 38 *Gorilla gorilla* (18/20)

45 Hommes anatomiquement modernes actuels et 21 fossiles : Cro Magnon 1, 3, Mladeč 1, Pataud, Rochereil, Nazlet Khater 2, Skhul 5, Song Terus, Téviec 8, 9, 16, Afalou Bou Rhummel et Taforalt (N=10)

23 homininés fossiles : Sts 5, KNM-WT 17000, KNM-ER 1813, 3733, 3883, OH 9, Broken Hill, LH 18, Ngandong 1, 7, 12, Sambungmacan 3, Ngawi, Liang Bua 1, Petralona, Gibraltar 1, Guattari, La Chapelle-aux-Saints, Saccopastore 1, La Ferrassie 1, La Quina H5, Spy 1 et 10

ASYMETRIES FRONTALES

ASYMETRIES OCCIPITALES



Synthèse et conclusions

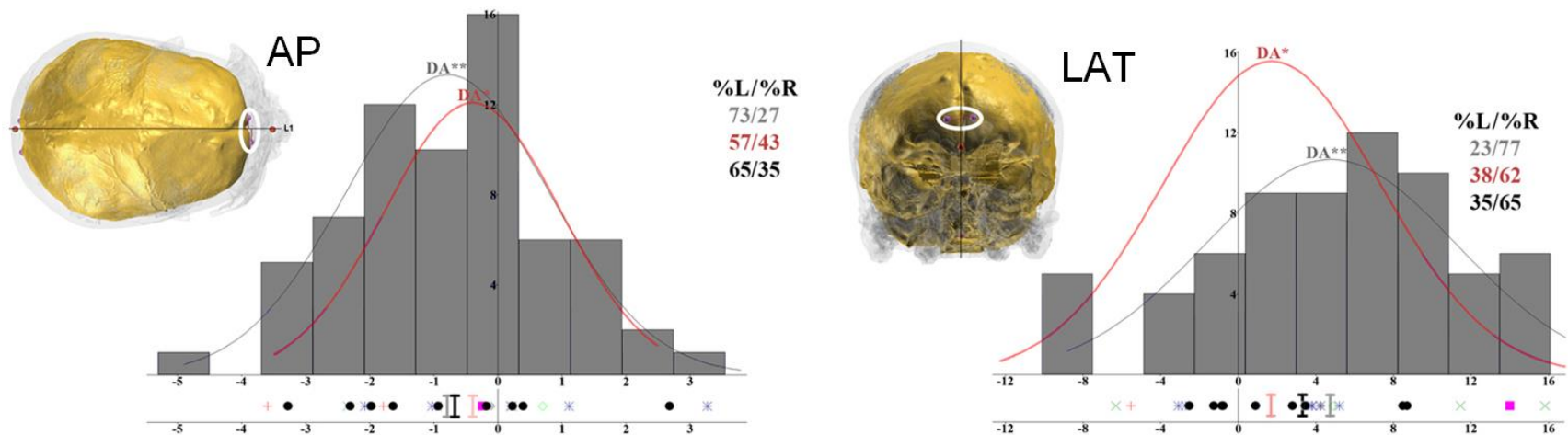
1- Homininés fossiles

Besoin de plus de matériel, mais sont plus proches des HAM que des grands singes

2- Schéma commun d'asymétrie de l'endocrâne chez les grands singes

Des similarités et quelques différences

Présence d'AD pour les composantes AP et latérale pour la pétalia occipitale !



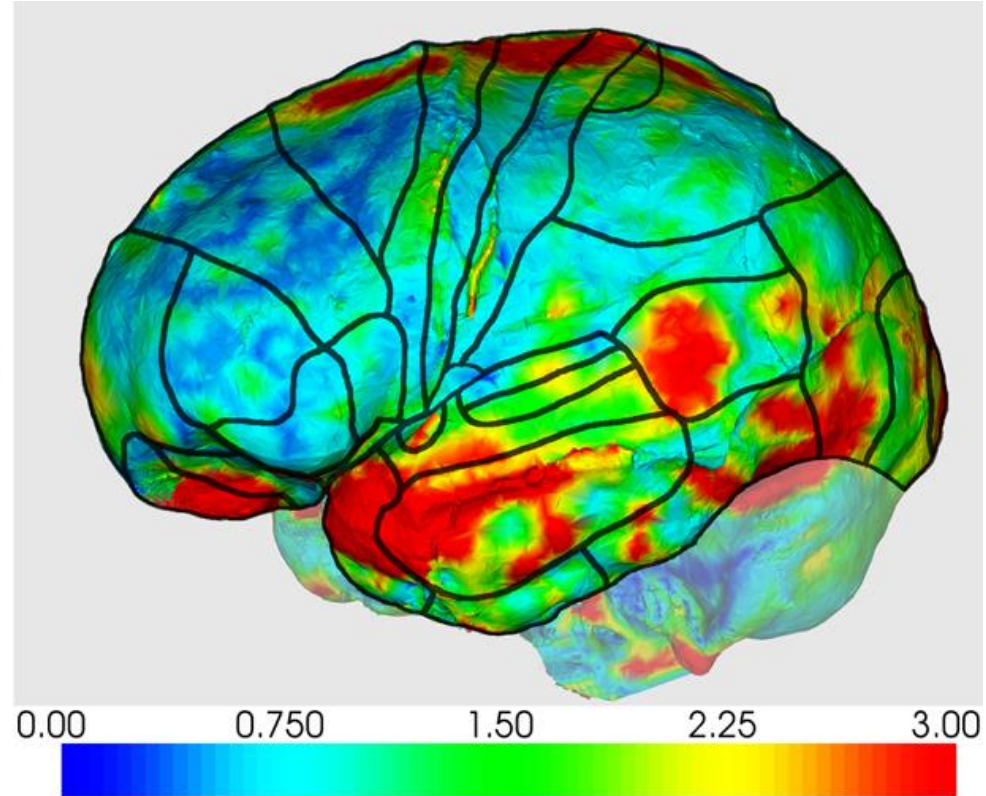
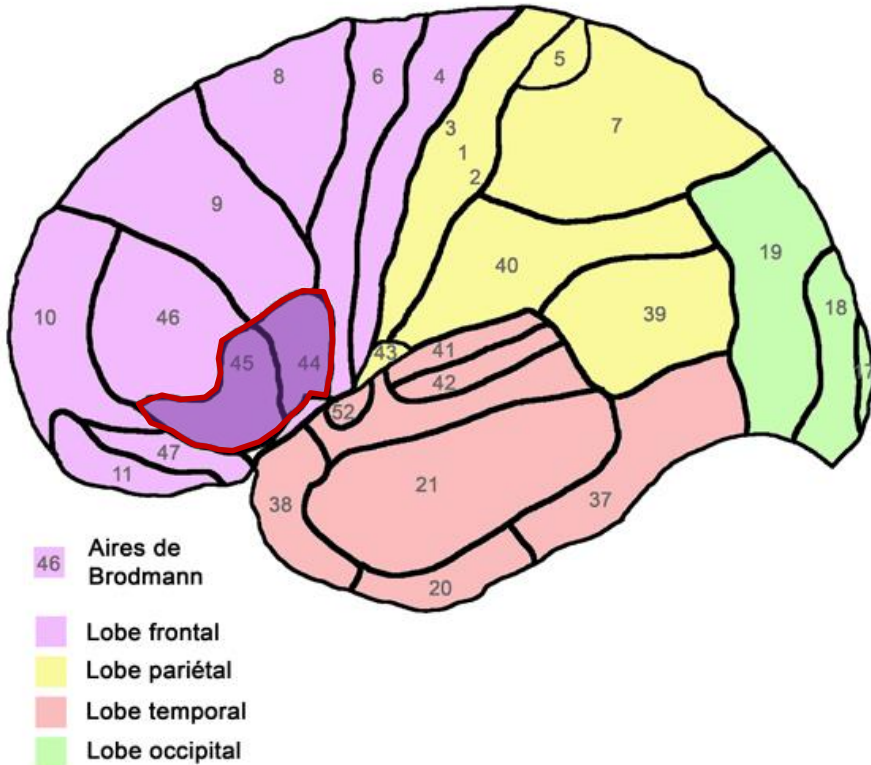
Implications pour la discussion des possibles relations entre les pétalias AP chez les homininés et les capacités fonctionnelles et comportementales

What is the Broca's area?



1861... Leborgne, « Tan »

Brodmann's cytoarchitectonic map



METHODS

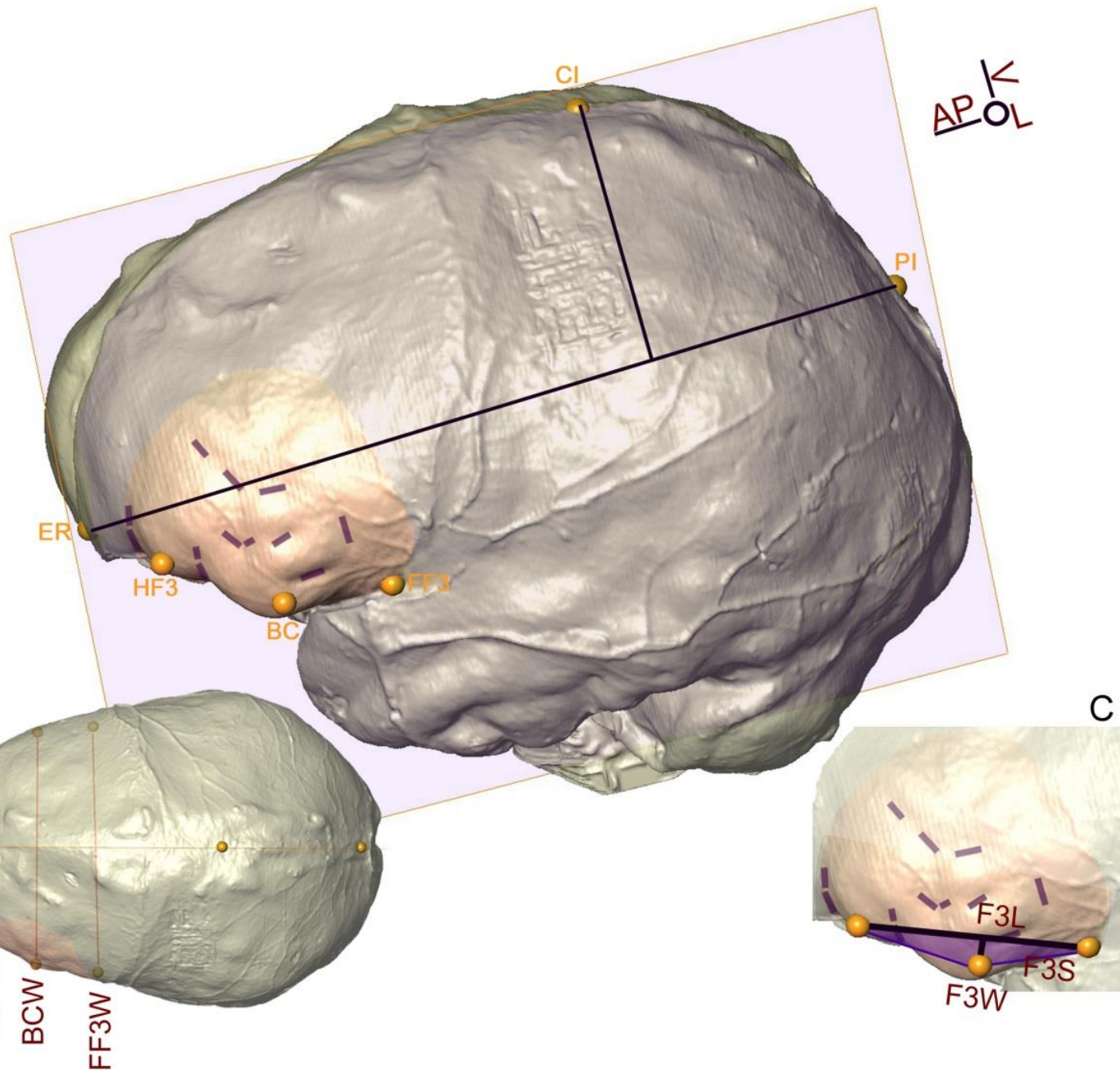
A

A: position of the landmarks used to delimitate the 3rd frontal convolution: the orbital part of the 3rd frontal convolution that corresponds to the anterior extension of the convolution (HF3), the point of maximal curvature of triangular part of the 3rd frontal convolution that characterize the lateral extension and bulging of the “Broca’s cap” (BC) and the upper point of the sylvian valley that is between the opercular part of the 3rd frontal convolution and the temporal lobe and therefore corresponds to the posterior extension of the 3rd frontal convolution (FF3); position of the 3 points used to define a plane in order to characterize bilateral asymmetries: the base of encephalic rostrum between left and right 1st frontal convolution in the midsagittal plane (ER), the intersection between the central sulci and the interhemispheric fissure (CI) and the intersection between the perpendicular sulci and the interhemispheric fissure (PI). The referential on the top right shows the orientation of the components of the asymmetries (method 1).

B

B: illustration of the widths of the frontal lobes at HF3 (HF3 width), at the level of the Broca’s cap (BC w), at FF3 (FF3 w).

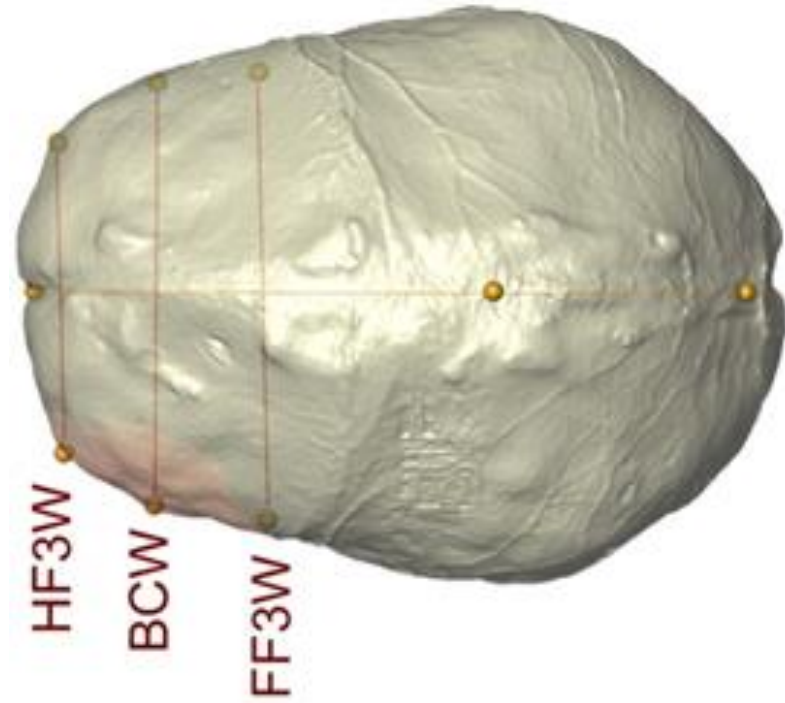
C: illustration of the antero-posterior extension of the 3rd frontal convolution (F3L), its width (F3W) and of the size (F3S) of the triangle defined by the 3 points delimitating the 3rd frontal convolution (C).



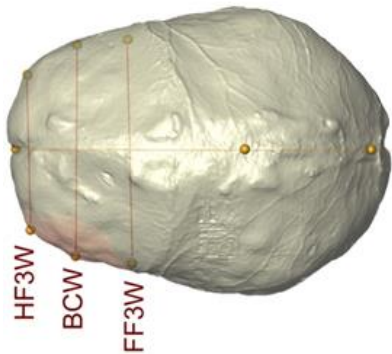
RESULTS

Width of the frontal lobes

This approach documents the bilateral distribution of pairs of anatomical points, but not of the bilateral variation in their size and shape because global shape of the other areas of the brain also influences these parameters.



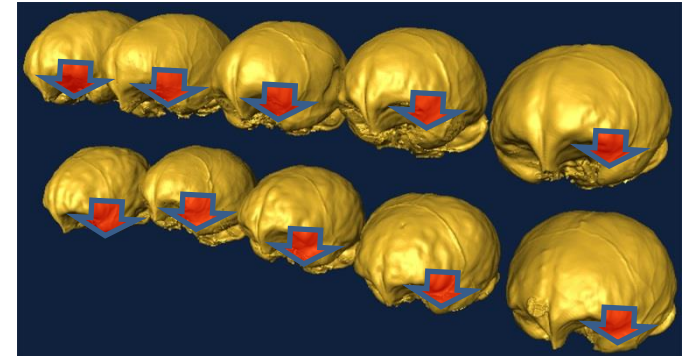
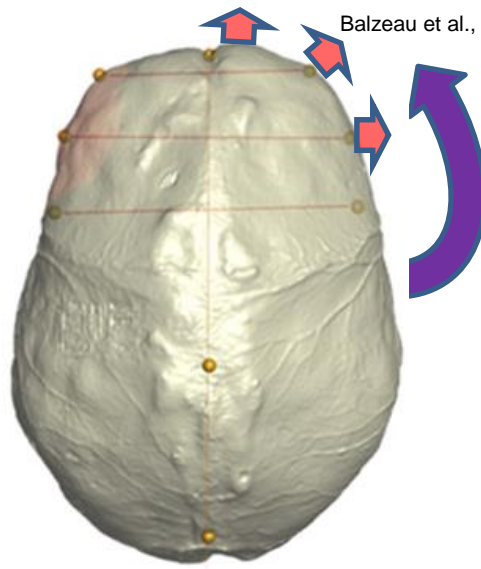
Width of the frontal lobes



		Neandertals (N=6)		73,4		65,6		104,6		93,5		104,7		93,6	
		Width head F3		Width Broca's cap		Width foot F3									
		absolute	relative	absolute	relative	absolute	relative	absolute	relative	absolute	relative	absolute	relative	absolute	relative
<i>Homo sapiens</i>	N	139													
	min	53,1	47,5	78,8	68,4	79,9	69,4								
	mean-SD	63,8	56,1	86,1	75,9	89,0	78,1								
	mean	70,4	62,1	92,3	81,4	97,2	85,8								
	mean+SD	77,0	68,1	98,4	86,9	105,4	93,4								
	max	90,6	81,5	109,8	98,8	118,6	106,8								
	V*	9,4	9,7	6,7	6,8	8,5	9,0								
<i>Pan paniscus</i>	N	35													
	min	39,2	58,6	55,9	81,7	58,4	86,6								
	mean-SD	46,2	66,8	60,2	87,2	63,4	91,6								
	mean	50,7	72,1	63,8	90,8	67,8	96,4								
	mean+SD	55,1	77,4	67,3	94,3	72,2	101,3								
	max	59,4	80,6	69,9	98,1	73,9	105,4								
	V*	8,9	7,4	5,6	4,0	6,5	5,1								
<i>Pan troglodytes</i>	N	36													
	min	45,8	64,2	62,7	89,2	59,2	87,6								
	mean-SD	52,8	73,3	65,9	91,3	65,1	90,6								
	mean	56,5	77,6	68,8	94,4	68,3	93,7								
	mean+SD	60,3	81,8	71,7	97,5	71,4	96,8								
	max	63,5	86,7	75,0	101,7	73,7	100,4								
	V*	6,7	5,5	4,2	3,3	4,6	3,3								

>

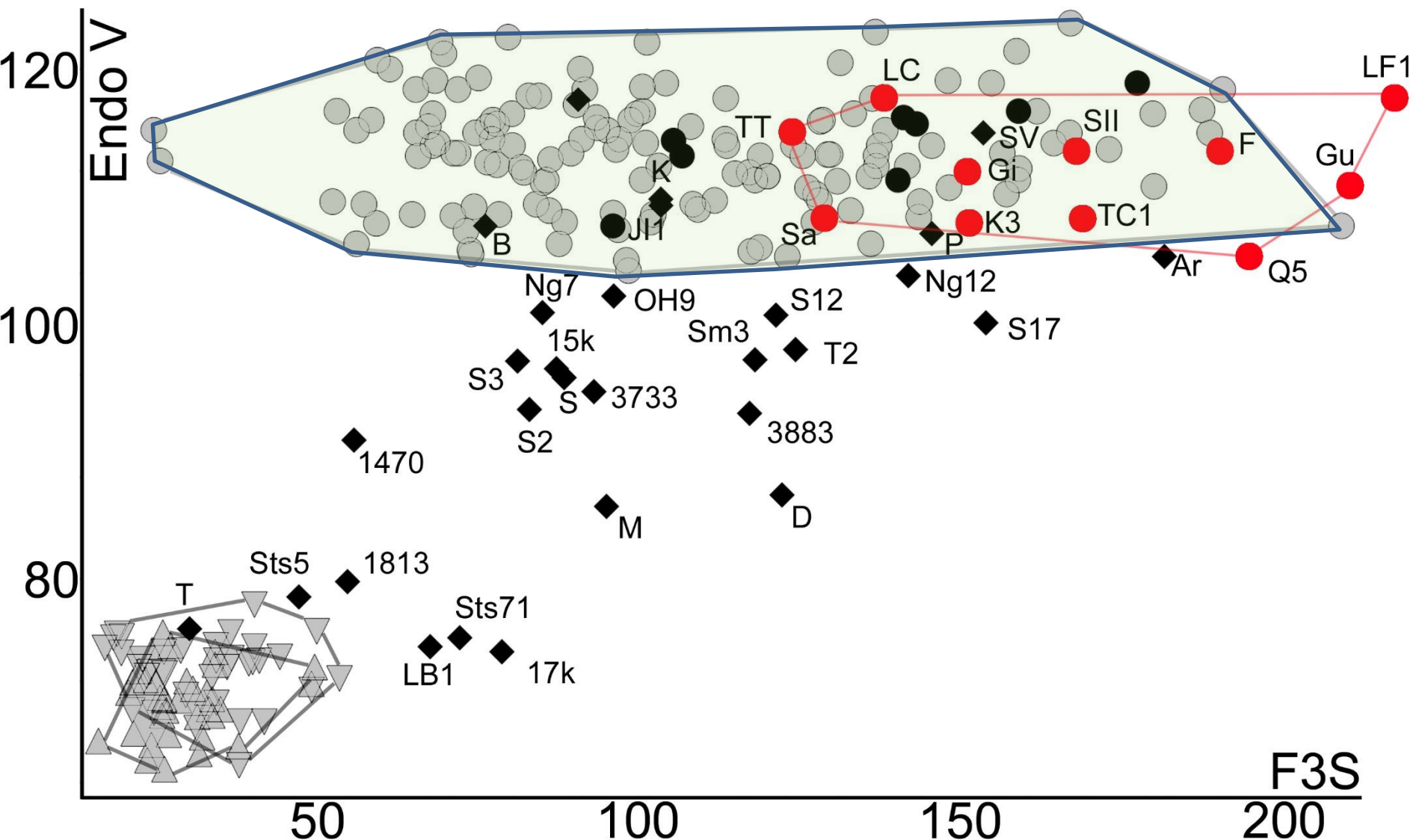
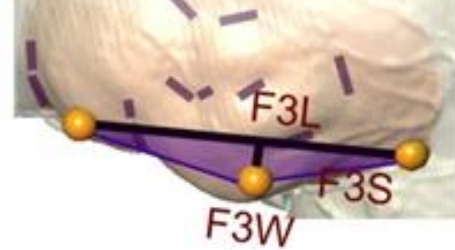
Asymmetries of the frontal lobes



		HF3			BC			FF3		
		AP	VERT	LAT	AP	VERT	LAT	AP	VERT	LAT
<i>Homo sapiens</i>	FA1	2,2	2,2	3,3	2,5	2,9	2,9	2,8	3,4	3,5
	DA	0,2	0,3	1,2 ***	-0,9 ***	0,7 *	1,8 ***	-1,1 ***	-0,5	2,3 ***
	FA4a	2,2	2,4	3,1	2,3	2,9	2,8	2,5	3,5	3,3
	Kurtosis	-0,3	0,7	-0,5	0,0	0,5	1,4 **	0,0	0,7	0,6
	Skew	0,1	-0,1	0,1	0,3	-0,6 **	0,5 *	0,2	-0,4	0,6 **
<i>Pan paniscus</i>	FA1	2,2	3,2	3,0	3,3	3,6	2,4	3,6	3,8	3,2
	DA	-1,0	-1,3	1,0	-1,9 **	-0,8	1,6	-2,9 ***	-0,3	2,4 ***
	FA4a	2,1	3,0	2,9	3,0	3,4	2,3	3,2	3,6	2,7
	Kurtosis	-0,5	0,3	-0,6	-0,3	-0,8	0,1	1,6 *	-0,6	-0,2
	Skew	0,2	0,5	0,3	-0,1	-0,1	0,9 *	-0,9 *	0,0	0,4
<i>Pan troglodytes</i>	FA1	1,5	3,4	1,8	2,0	29,9	2,4	2,5	6,1	1,9
	DA	-0,5	-1,9 *	0,3	-0,4	-29,8 ***	-0,4	-1,9 ***	-6,1 ***	0,3
	FA4a	1,5	3,9	2,1	1,9	3,8	2,3	2,1	2,7	1,9
	Kurtosis	-0,2	6,6 ***	6,1 ***	0,3	0,6	0,4	6,6 ***	0,1	0,5
	Skew	-0,4	-2 ***	1,6 ***	0,2	-0,2	-0,4	1,5 ***	-0,3	0,3

* indicates a p value <0.05, **<0.01, ***<0.001 after sequential Bonferroni procedure for correction for multiple tests.

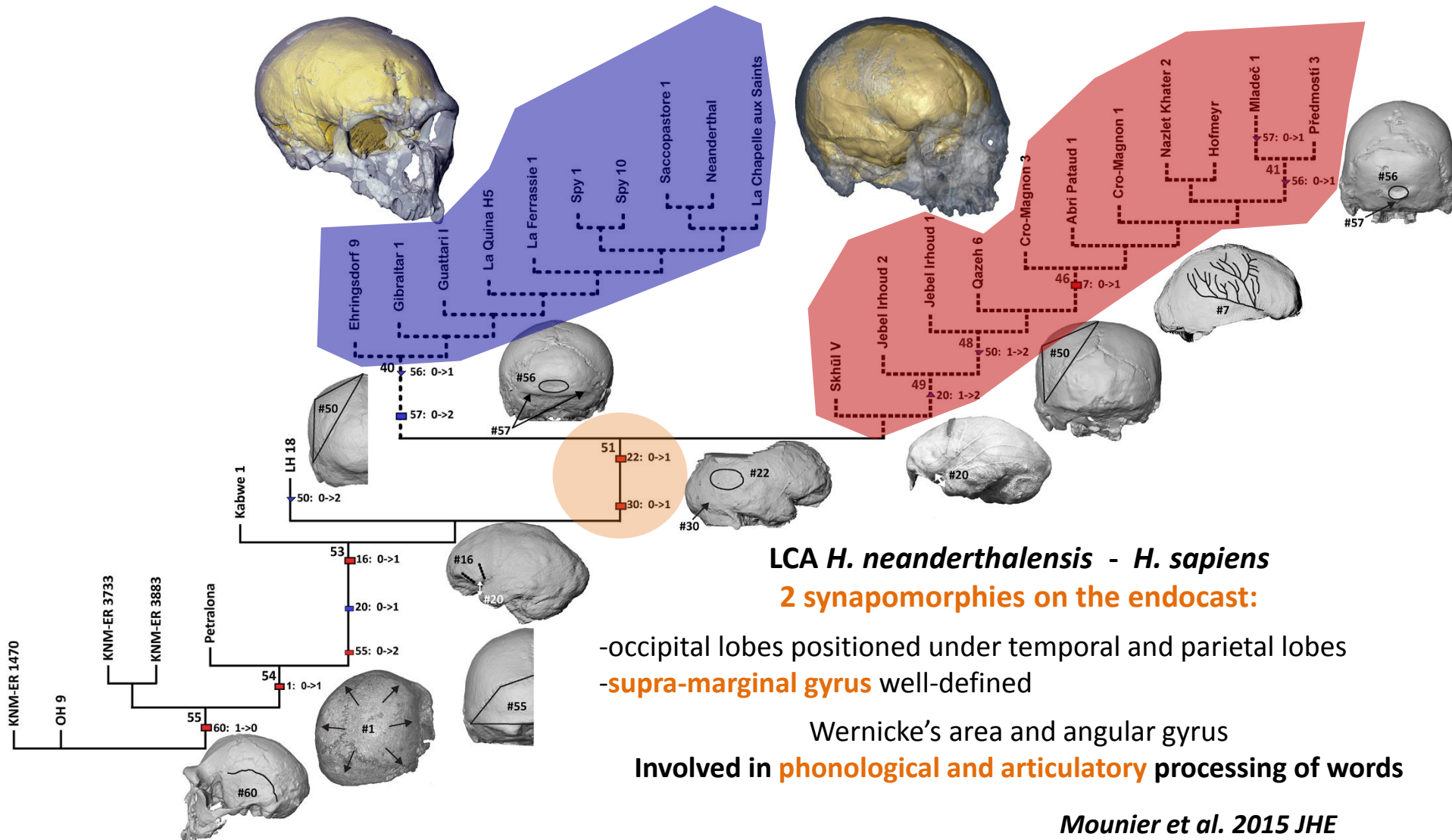
Size of the « Broca's cap »

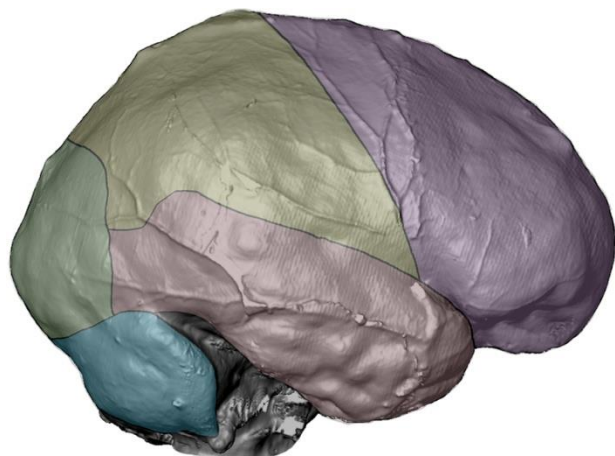
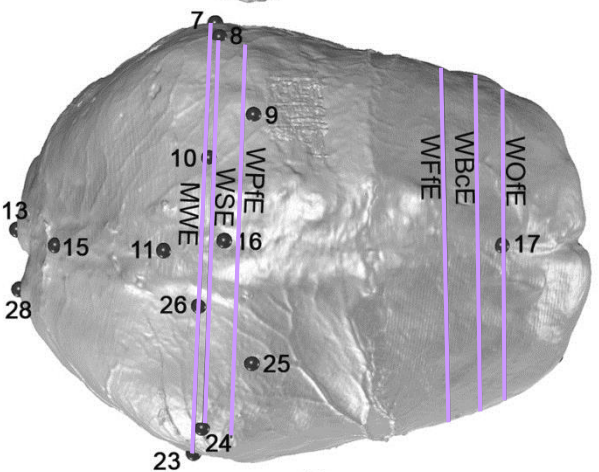
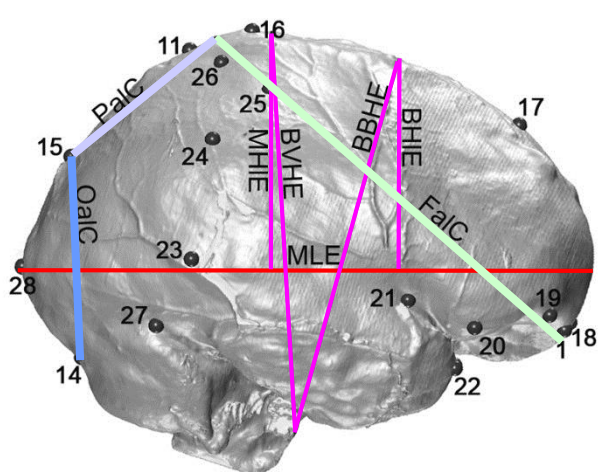


Evolution of language: major hypotheses

Great Leap Forward II

Anatomy – Brain

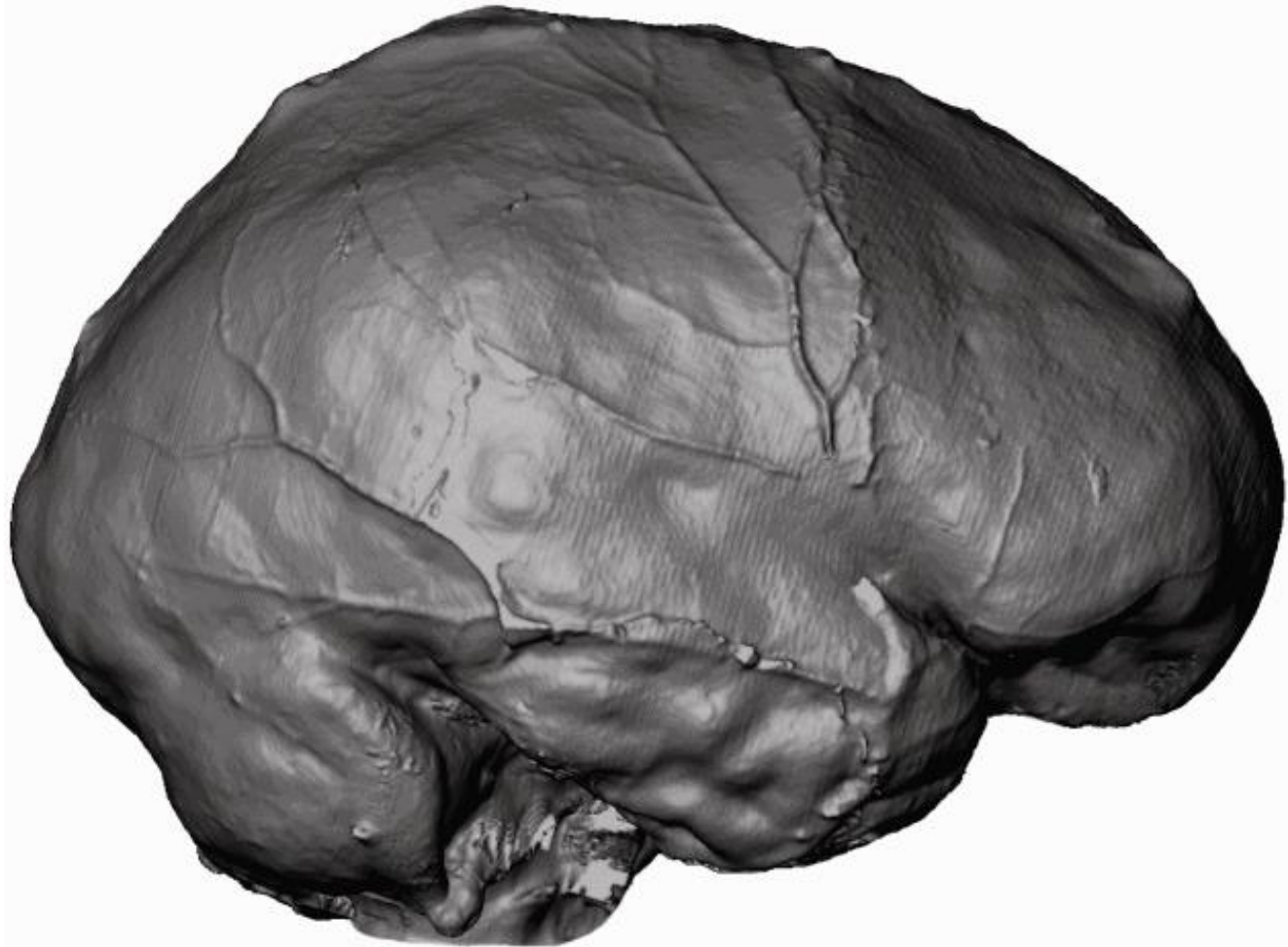
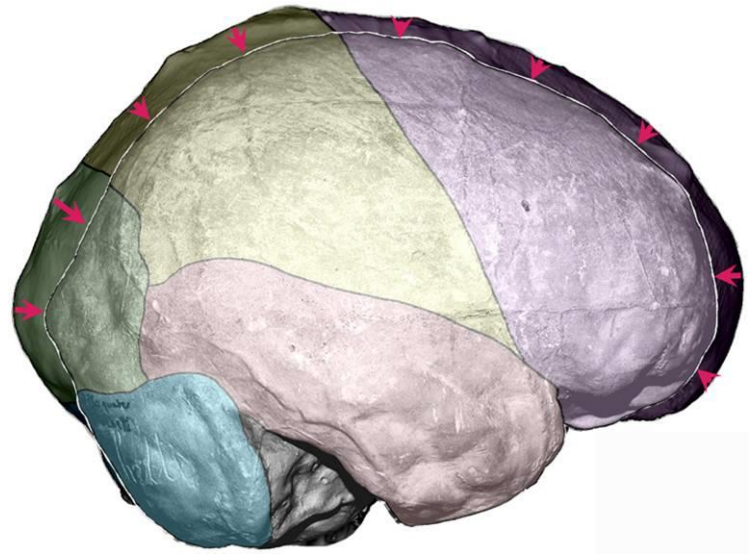


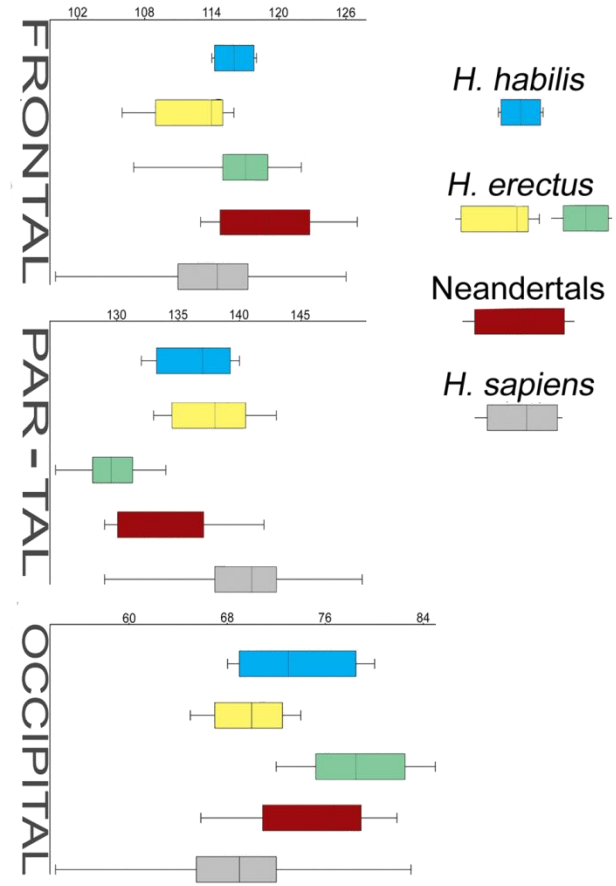
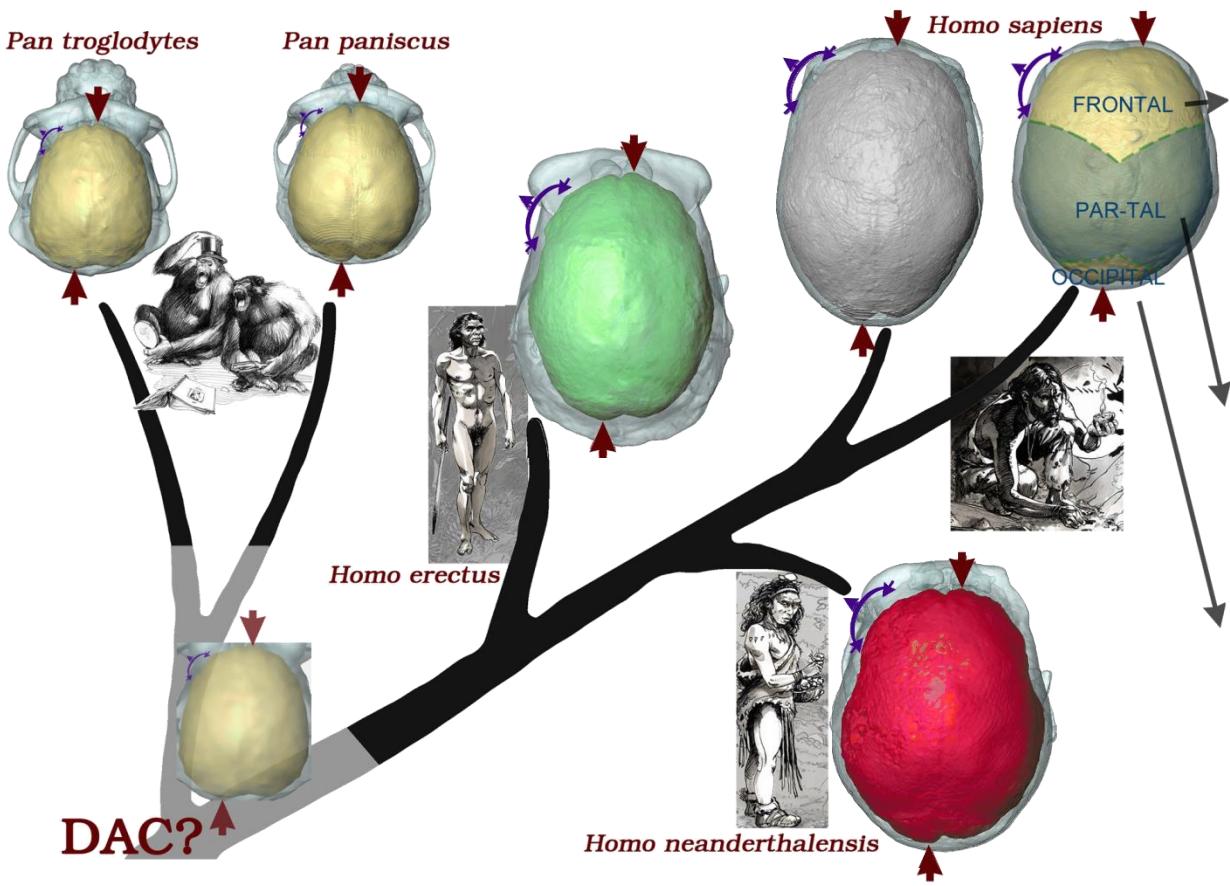
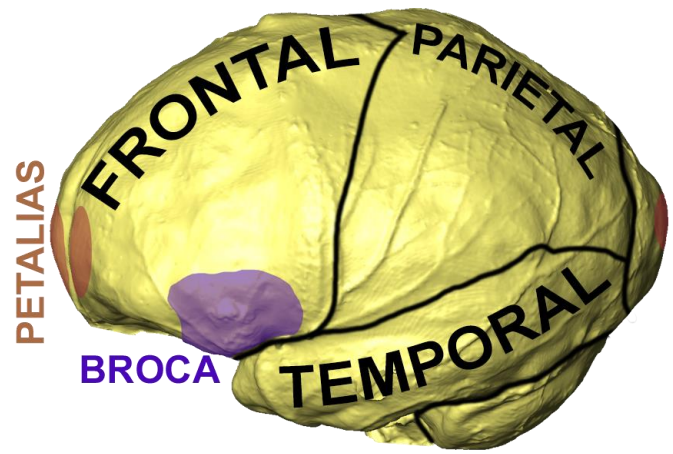


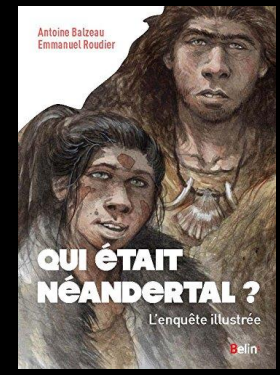
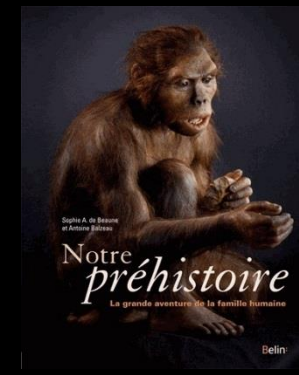
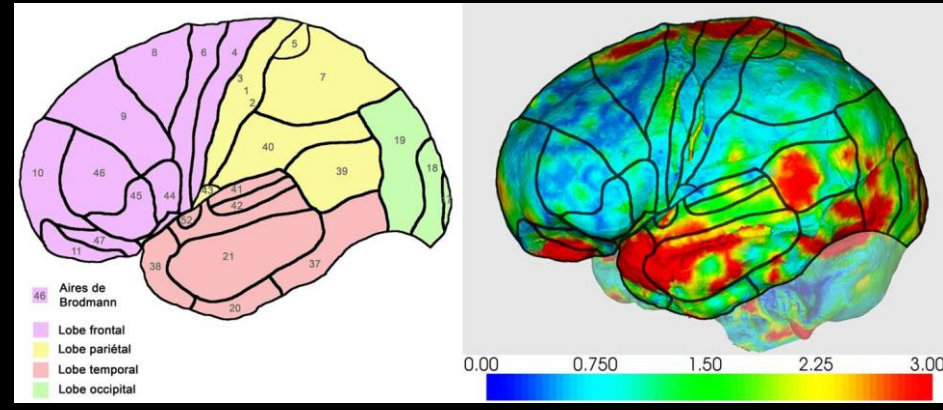
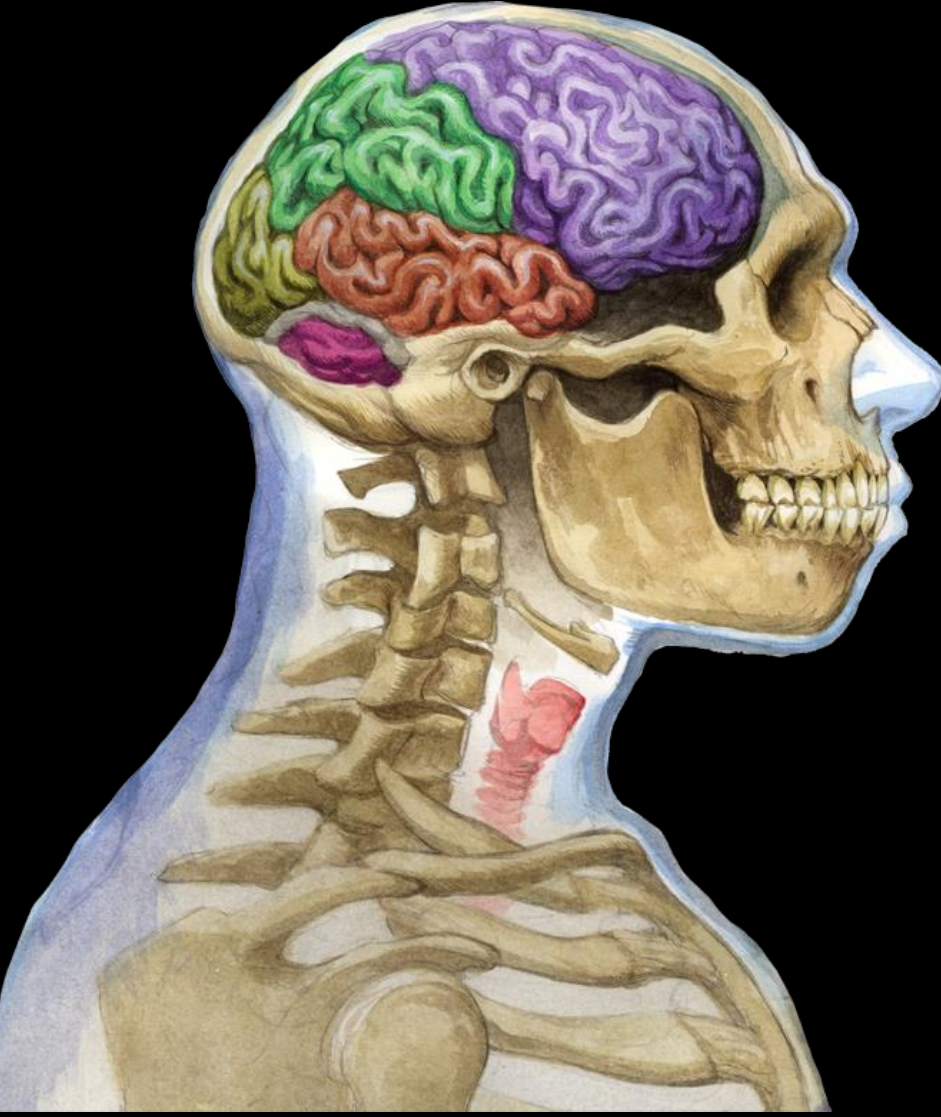
	MLE	MWE	WSE	WPfE	WbCe	WofE	WfE	Wcereb	BBHE	BVHE	MHIE	BHIE	
UP AMH	N	13	13	14	13	11	9	10	8	8	7	11	12
	V*	3.9	4.4	5.0	4.8	4.4	3.3	5.6	5.8	4.3	5.0	7.9	5.9
	Min	15.1	10.8	10.7	10.7	8.9	7.1	9.2	9.0	10.3	10.6	6.0	5.5
	Mean-SD	15.3	11.3	10.9	10.9	8.9	7.2	9.5	9.2	10.5	10.6	6.2	5.6
	Mean	15.9	11.9	11.5	11.5	9.3	7.5	10.0	9.7	11.0	11.2	6.8	6.0
	Mean+SD	16.5	12.4	12.0	12.0	9.7	7.7	10.6	10.2	11.4	11.7	7.3	6.3
Max	17.0	12.9	12.5	12.5	10.0	7.9	10.9	10.6	11.8	12.2	7.8	6.5	
Extant AMH	N	102	102	102	102	102	102	102	102	101	101	101	101
	V*	4.1	4.5	3.9	4.2	5.7	12.8	5.3	4.8	3.9	3.5	10.9	11.9
	Min	13.5	10.6	10.3	10.2	8.1	5.9	8.8	8.1	9.2	9.9	4.6	4.1
	Mean-SD	14.3	11.3	11.1	10.9	8.6	6.6	9.6	8.8	10.2	10.5	5.2	4.5
	Mean	14.9	11.9	11.5	11.3	9.1	7.5	10.1	9.2	10.6	10.8	5.8	5.1
	Mean+SD	15.5	12.4	11.9	11.8	9.7	8.5	10.7	9.7	11.0	11.2	6.4	5.7
Max	16.0	13.1	12.7	12.4	10.5	9.9	11.5	10.3	11.5	11.8	7.5	6.8	
perm. t(bc) p	***	ns	ns	ns	ns	ns	ns	*	*	*	***	***	
%MeanVar	7	0	0	1	2	0	-1	5	4	3	16	16	

	FC	PC	OC	
UP AMH	N	13	13	
	V*	4.05	7.05	8.27
	Min	10.59	5.17	5.25
	Mean-SD	10.91	5.58	5.48
	Mean	11.36	6.00	5.96
	Mean+SD	11.81	6.42	6.45
Max	12.16	6.92	6.80	
Extant AMH	N	102	102	102
	V*	4.34	11.03	8.65
	Min	9.48	4.58	4.12
	Mean-SD	10.22	5.72	4.66
	Mean	10.69	6.43	5.10
	Mean+SD	11.15	7.14	5.54
Max	12.08	7.72	6.18	
perm. t(bc) p	***	*	***	
%MeanVar	6	-7	17	

	Frontal lobes	Parietal lobes	Occipital lobes	cerebellar lobes	
UP AMH	N	11	7	9	7
	V*	4.33	4.97	6.37	6.38
	Min	0.78	0.95	0.49	0.44
	Mean-SD	0.82	0.95	0.49	0.45
	Mean	0.85	1.00	0.52	0.48
	Mean+SD	0.89	1.05	0.56	0.51
Max	0.90	1.10	0.59	0.52	
Extant AMH	N	98	98	98	97
	V*	4.02	2.95	7.98	5.38
	Min	0.71	0.91	0.38	0.43
	Mean-SD	0.77	0.96	0.45	0.48
	Mean	0.81	0.99	0.49	0.50
	Mean+SD	0.84	1.02	0.52	0.53
Max	0.88	1.06	0.57	0.56	
perm. t(bc) p	***	ns	**	*	
%MeanVar	6	1	8	5	







<http://antoinebalzeau.fr/>